arXiv:1606.03822v3 [cond-mat.str-el] 25 Oct 2016

Microscopic theory of Dzyaloshinsky-Moriya interaction in pyrochlore oxides with spin-orbit coupling

Naoya Arakawa*
Center for Emergent Matter Science (CEMS), RIKEN, Wako, Saitama 351-0198, Japan
(Dated: October 26, 2016)

Pyrochlore oxides show several fascinating phenomena, such as the formation of heavy fermions and the thermal Hall effect. Although a key to understanding some phenomena may be the Dzyaloshinsky-Moriya (DM) interaction, its microscopic origin is unclear. To clarify the microscopic origin, we constructed a t_{2g}-orbital model with the kinetic energy, the trigonal-distortion potential, the multiorbital Hubbard interactions, and the LS coupling, and derived the low-energy effective Hamiltonian for a d^1 Mott insulator with the weak LS coupling. We first show that lack of the inversion center of each nearest-neighbor V-V bond causes the odd-mirror interorbital hopping integrals. Those are qualitatively different from the even-mirror hopping integrals, existing even with the inversion center. We next show that the second-order perturbation using the kinetic terms leads to the ferromagnetic and the antiferromagnetic superexchange interactions, whose competition is controllable by tuning the Hubbard interactions. Then, we show the most important result: the third-order perturbation terms using the combination of the even-mirror hopping integral, the odd-mirror hopping integral, and the LS coupling causes the DM interaction due to the mirror-mixing effect, where those hopping integrals are necessary to obtain the antisymmetric kinetic exchange and the LS coupling is necessary to excite the orbital angular momentum at one of two sites. We also show that the magnitude and sign of the DM interaction can be controlled by changing the positions of the O ions and the strength of the Hubbard interactions. We discuss the advantages in comparison with the phenomenological theory and Moriya's microscopic theory, applicability of our mechanism, and the similarities and differences between our case and the strong-LS-coupling case.

I. INTRODUCTION

The pyrochlore oxides[1] show several fascinating phenomena, and the electronic states of some pyrochlore oxides are categorized into a t_{2g}-orbital system with the tetrahedral sublattice structure under the trigonal-distortion potential. One of the fascinating phenomena is the formation of heavy fermions: in the paramagnetic metallic state of LiV_2O_4, the low-temperature coefficient of the electronic specific heat becomes about 0.42J/mol-K^2, indicating the largest mass enhancement in transition-metal compounds[2]. Another is the thermal-Hall effect: in the ferromagnetic (FM) Mott insulating state of $Lu_2V_2O_7$, the temperature gradient leads to the heat flow perpendicular to it[3]. As an example of the pyrochlore oxides, let us consider the pyrochlore vanadates. The V ions form a network of corner-sharing tetrahedra, and each V ion and six O ions form a octahedron[1]; four V ions of a tetrahedron correspond to the sublattice degrees of freedom [see Fig. 1(a)], and the nearest-neighbor V ions are connected by an O ion. Then, the t_{2g} orbitals of the V ions, i.e., the d_{xz}, d_{yz}, and d_{xy} orbitals, give the main contributions to the bands near the Fermi level[4–6]. In addition, the trigonal distortion reduces the symmetry group around a V ion, and splits the t_{2g} orbitals into the singlet a_{1g} orbital and the doublet e_g^+ and e_g^- orbitals [Fig. 1(b)]; the a_{1g} orbital and the e_g^+ and e_g^- orbitals correspond to the basis functions of the A_{1g} and the E_g irreducible representations, respectively.

A key quantity to understand some properties of the pyrochlore oxides may be the Dzyaloshinsky-Moriya (DM) interaction. The DM interaction[7,8] has been believed to be realized in the pyrochlore oxides because of lack of the inversion center in each nearest-neighbor V-V bond of a tetrahedron[9]. This realization was pointed out by the phenomenological argument[9]: the authors of Ref. 9 showed the possible components of the DM interaction without the inversion center. This result may be correct because the fitting of the spin-wave dispersions obtained in the inelastic neutron scattering[10] for $Lu_2V_2O_7$ suggests the finite DM interaction, although this fitting was carried out in a rough model and there is a controversy about the value of the DM interaction for $Lu_2V_2O_7$[11]. In addition, the results for $CdCr_2O_4$[12,13] and $Sm_2Ir_2O_7$[14] suggest the finite DM interaction in pyrochlore oxides. Moreover, the emergence of the thermal-Hall effect may support the existence of the DM interaction because the necessity of the DM interaction was shown in several previous theoretical studies[3,15,16], although these theoretical studies neglected the sublattice degree of freedom in treating the DM interaction.

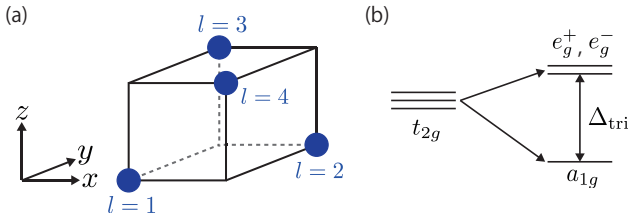

FIG. 1: Schematic pictures of (a) a tetrahedron of four V ions (blue circles), and (b) the splitting of the t_{2g} orbitals under the trigonal-distortion potential, $\Delta_{\rm tri}$.

It is important to clarify the microscopic origin of the DM interaction in pyrochlore oxides. This is because if we clarify the microscopic origin, we can understand the following four points. First, we can understand whether some components of the DM interaction are truly finite. That cannot be analyzed by the phenomenological argument[7] because the phenomenological theory just determines the permissible components from a symmetrical point of view. On the other hand, the microscopic theory, such as Moriya's microscopic theory[8], determines the coefficients of the DM interaction, expressed in terms of the parameters of the noninteracting Hamiltonians and the interacting Hamiltonian. Second, the microscopic theory can clarify how the electronic structure of pyrochlore oxides leads to the DM interaction and how the magnitude and sign of the DM interaction are controlled by tuning the parameters of the system. Third, if we estimate the parameters of the noninteracting Hamiltonians and the interacting Hamiltonian by first-principles calculations such as the local-density approximation, we can determine the DM interaction appropriately including the material dependence of the electronic structure. Fourth, if we proceed to study the phenomena that may be related to the DM interaction, we can more deeply understand the physics of those phenomena.

To clarify the microscopic origin of the DM interaction in pyrochlore oxides, we constructed a t_{2g}-orbital model with the appropriate treatments of the orbital degrees of freedom, lack of the inversion center of each V-V bond, the trigonal-distortion potential, the multiorbital electron correlation, and the spin-orbit coupling (SOC), and derived the low-energy effective Hamiltonian for a d^1 Mott insulator in the similar way for Moriya's microscopic theory[8]. We first show that due to lack of the inversion center, the indirect hopping integrals through the O $2p$ orbitals not only modify the values of the direct hopping integrals, which are even-mirror, but also induce the odd-mirror hopping integrals, which are missing only in the direct hopping integrals. The appearance of the odd-mirror hopping integrals is a microscopic effect of lack of the inversion center. We next show the FM and the antiferromagnetic (AF) superexchange interactions, derived by the second-order perturbation using two even-mirror hopping integrals or two odd-mirror hopping integrals. As the most important result, we show that the DM interaction arises from the mirror-mixing effect in the third-order perturbation using the combination of the even-mirror hopping integral, the odd-mirror hopping integral, and the LS coupling. In this mirror-mixing effect, the role of those hopping integrals is to induce the antisymmetric kinetic exchange, and the role of the LS coupling is to activate the orbital angular momentum at one of two sites. Those two roles are vital to get the DM-type antisymmetric exchange interactions in the weak SOC because in the nonperturbed states, the orbital angular momenta are quenched and because the combination of the antisymmetries of the kinetic exchange and the orbital angular momenta of two sites is necessary. In addition, from the equation of the coefficient of the DM interaction, we deduce how to control its magnitude and sign by tuning the parameters of the model. Then, we compare the present microscopic theory with the phenomenological theory[9] for the DM interaction in pyrochlore oxides, Moriya's microscopic theory[8], and the previous microscopic theory[17] in the strong SOC, and reveal the similarities and differences. We also argue the applicability of our mechanism to the DM interaction in solids with the weak SOC.

In the remaining part of this paper, we explain how to construct the appropriate t_{2g}-orbital model for pyrochlore oxides, derive the low-energy effective Hamiltonian for a d^1 Mott insulator with the weak SOC, discuss the correspondences between our theory and several previous theories about the DM interaction and the applicability of our mechanism, and give the summary of our achievements. The construction of the t_{2g}-orbital model is explained in Sec. II. The model consists of four Hamiltonians, and the detail of each Hamiltonian is explained in each of Secs. II A, II B, II C, and II D, respectively. The low-energy effective Hamiltonian is derived in Sec. III. We derive the second-order perturbation terms in Sec. III A, and the third-order perturbation terms in Sec. III B. We also show the results of the rough estimations of the sign of the second-order terms, the ratio of the leading third-order term to the second-order terms, and the ratio of the secondary third-order term to the leading term in Sec. III A, III B 1, and III B 2, respectively. The correspondences with the previous theories and the applicability are discussed in Sec. IV. We summarize our results and their meanings in Sec. V.

II. MODEL

As an effective model of pyrochlore oxides, we introduce the following total Hamiltonian, $\hat{H}_{\rm tot}$, with the chemical potential term, $\mu\hat{N}$:

$$\hat{H}_{\rm tot} - \mu\hat{N} = \hat{H}_{\rm KE} + \hat{H}_{\rm tri} + \hat{H}_{\rm int} + \hat{H}_{LS} - \mu\hat{N}. \quad (1)$$

Here $\hat{H}_{\rm KE}$, $\hat{H}_{\rm tri}$, $\hat{H}_{\rm int}$, and $\hat{H}_{LS}$ represent the kinetic energy of the t_{2g}-orbital electrons, the trigonal-distortion potential, the t_{2g}-orbital Hubbard interactions, the SOC for the t_{2g}-orbital electrons, respectively, and $\hat{N}$ is

$$\hat{N} = \sum_{\boldsymbol{i}} \sum_{a=d_{xz},d_{yz},d_{xy}} \sum_{s=\uparrow,\downarrow} \hat{c}^{\dagger}_{\boldsymbol{i}as}\hat{c}_{\boldsymbol{i}as}, \quad (2)$$

with the site index $\boldsymbol{i}$, the orbital index a, and the spin index s. $\hat{H}_{\rm KE}$, $\hat{H}_{\rm tri}$, $\hat{H}_{\rm int}$, and $\hat{H}_{LS}$ are explicitly shown in Secs. II A, II B, II C, and II D, respectively. μ is so determined that the electron number per site is 1 for $Lu_2V_2O_7$ or 1.5 for LiV_2O_4 for example.

In comparison with several previous theoretical studies[18–21] of the pyrochlore oxides, a new point of this effective model is an appropriate treatment of lack of the

inversion center of each nearest-neighbor V-V bond, resulting in an appropriate treatment of orbital and sublattice degrees of freedom (for the details see Sec. II A). It should be noted that although there is a previous study[22] about the effects of lack of the inversion center on the hopping integrals for V ions, its authors did not consider the hopping integrals between the t_{2g}-orbital electrons arising from lack of the inversion center.

In the following, we use the unit $\hbar = c = 1$.

A. $\hat{H}_{\mathrm{KE}}$

To derive the kinetic energy of the t_{2g}-orbital electrons for pyrochlore oxides, we consider the nearest-neighbor hopping integrals for the V t_{2g} orbitals and derive these by adopting the Slater-Koster method[23] to not only the direct hoppings but also the indirect hoppings through the O $2p$ orbitals. As we derive below, $\hat{H}_{\mathrm{KE}}$ is given by

$$\begin{aligned}\hat{H}_{\mathrm{KE}} =& \hat{H}_0 + \hat{H}_{\mathrm{odd}} \\ =& \sum_{<\boldsymbol{i},\boldsymbol{j}>} \sum_{a,b=d_{xz},d_{yz},d_{xy}} \sum_{s=\uparrow,\downarrow} t^{(\mathrm{even})}_{\boldsymbol{ij};ab} \hat{c}^{\dagger}_{\boldsymbol{i}as} \hat{c}_{\boldsymbol{j}bs} \\ &+ \sum_{<\boldsymbol{i},\boldsymbol{j}>} \sum_{a,b=d_{xz},d_{yz},d_{xy}} \sum_{s=\uparrow,\downarrow} t^{(\mathrm{odd})}_{\boldsymbol{ij};ab} \hat{c}^{\dagger}_{\boldsymbol{i}as} \hat{c}_{\boldsymbol{j}bs}, \end{aligned} \tag{3}$$

where $\sum_{<\boldsymbol{i},\boldsymbol{j}>}$ represents the summation between the nearest-neighbor sites, $\hat{H}_0$ represents the even-mirror hopping integrals, $t^{(\mathrm{even})}_{\boldsymbol{ij};ab}$, existing even with the inversion center of each nearest-neighbor V-V bond, and $\hat{H}_{\mathrm{odd}}$ represents the odd-mirror hopping integrals, $t^{(\mathrm{odd})}_{\boldsymbol{ij};ab}$, appearing only with lack of the inversion center. The word "even-mirror" or "odd-mirror" mean that the mirror symmetry about the plane including the nearest-neighbor sites is even or odd, respectively; e.g., for a xy plane including sublattices 1 and 2, the hopping integral between the d_{xy} orbitals is even about the mirror symmetry of the xy plane (i.e., $x \to x$, $y \to y$, and $z \to -z$) and the hopping integral between the d_{xz} and d_{xy} orbitals is odd because the former and latter behave like $xy \times xy \propto x^2y^2z^0$ and $xz \times xy \propto x^2y^1z^1$, respectively.

We first derive the contributions from the direct hoppings between nearest-neighbor V ions. We derive only the hopping integrals between V ions at sublattices 1 and 2 [i.e. $l = 1$ and 2 in Fig. 1(a)] because the others can be obtained from these by permuting the coordinates x, y, and z, defined in Fig. 1(a). For example, the direct hopping integrals between sublattices 1 and 3 are obtained by replacing x, y, and z in the direct hopping integrals between sublattices 1 and 2 by y, z, and x, respectively, e.g., $t^{(\mathrm{direct})}_{d_{xz}3d_{yz}1} = t^{(\mathrm{direct})}_{d_{yz}2d_{xy}1}$. Adopting the Slater-Koster method[23] to the direct hopping integrals between V ions at sublattices 1 and 2, which are located at $(x, y, z) = (0, 0, 0)$ and $(1, 1, 0)$, respectively, we can express the hopping integrals for the t_{2g}-orbital electrons in terms of three Slater-Koster parameters, $V_{dd\sigma}$, $V_{dd\pi}$, and $V_{dd\delta}$:

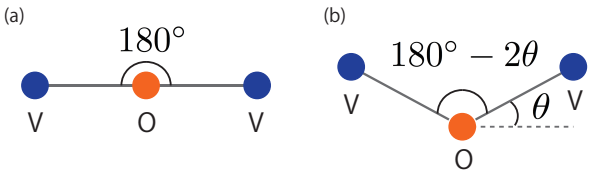

FIG. 2: Schematic pictures of a V-O-V bond (a) with and (b) without the inversion center. Blue and orange circles denote V and O ions, respectively. This angle deviation breaks the mirror symmetry about the plane including the V ions.

$$t^{(\mathrm{direct})}_{d_{xy}2d_{xy}1} = \frac{3}{4}V_{dd\sigma} + \frac{1}{4}V_{dd\delta}, \tag{4}$$

$$t^{(\mathrm{direct})}_{d_{xz}2d_{xz}1} = \frac{1}{2}V_{dd\pi} + \frac{1}{2}V_{dd\delta}, \tag{5}$$

$$t^{(\mathrm{direct})}_{d_{yz}2d_{yz}1} = t^{(\mathrm{direct})}_{d_{xz}2d_{xz}1}, \tag{6}$$

$$t^{(\mathrm{direct})}_{d_{xy}2d_{yz}1} = 0, \tag{7}$$

$$t^{(\mathrm{direct})}_{d_{xy}2d_{xz}1} = 0, \tag{8}$$

$$t^{(\mathrm{direct})}_{d_{yz}2d_{xz}1} = \frac{1}{2}V_{dd\pi} - \frac{1}{2}V_{dd\delta}, \tag{9}$$

$$t^{(\mathrm{direct})}_{d_{xz}2d_{yz}1} = t^{(\mathrm{direct})}_{d_{yz}2d_{xz}1}, \tag{10}$$

$$t^{(\mathrm{direct})}_{d_{xz}2d_{xy}1} = 0, \tag{11}$$

$$t^{(\mathrm{direct})}_{d_{yz}2d_{xy}1} = 0. \tag{12}$$

Since all the finite direct hopping integrals are even about the mirror symmetry of the xy plane, the direct hoppings lead only to the even-mirror hopping integrals.

We next derive the contributions from the indirect hoppings through the O $2p$ orbitals. As we will show below, if we appropriately treat the effect of lack of the inversion center of each nearest-neighbor V-V bond, the indirect hoppings lead to the odd-mirror hopping integrals, which are missing in the direct hoppings. The position of the O ion of each V-O-V bond deviates from the center; i.e., each V-O-V angle deviates from 180° [compare Figs. 2(a) and 2(b)]. In addition, this deviation results in the four-sublattice structure of a tetrahedron because V ions at sublattices 1, 2, 3, and 4 are different from each other; for example, if we compare the lower layer of a tetrahedron including sublattices 1 and 2 with the upper layer including sublattices 3 and 4, we see the difference between the V ions in the lower layer and the upper layer because the O ion for V ions of sublattices 1 and 2 (sublattices 3 and 4) is located below the lower layer (above the upper layer). To show that the indirect hoppings lead to the odd-mirror hopping integrals only with lack of the inversion center of each nearest-neighbor V-V bond, we consider the case in which each V-O-V angle slightly deviates from 180°, i.e., the angle is $180° - 2\theta$ [see Fig. 2(b)], and derive the indirect hopping integrals between V ions at sublattices 1 and 2 through the O ion. Because of the same reason for the derivation of the direct hopping

integrals, we derive only the hopping integrals between sublattices 1 and 2. Since the indirect nearest-neighbor hopping integrals, $t_{a2b1}^{(\mathrm{indirect})}$, are given by

$$t_{a2b1}^{(\mathrm{indirect})} = \sum_{A=p_x,p_y,p_z} \frac{V_{a2A}V_{Ab1}}{\Delta_{pd}}, \tag{13}$$

we need to derive the hybridizations between V t_{2g} orbitals and O $2p$ orbitals, V_{a2A} and V_{Ab1}, for a V-O-V bond including sublattices 1 and 2 by using the Slater-Koster method[23]. In Eq. (13), we have neglected the orbital and θ dependence of Δ_{pd}, the crystalline-electric-field energy difference between V t_{2g} orbitals and O $2p$ orbitals, because this simplification is sufficient for our purpose, i.e., showing the appearance of the odd-mirror hopping integrals. V_{Ab1} are obtained by adopting the Slater-Koster method to the indirect hopping processes between the V ion at $(x, y, z) = (0, 0, 0)$ and the O ion at $(x, y, z) = (\frac{1}{2}, \frac{1}{2}, -\frac{1}{2}\tan\theta)$ with two Slater-Koster parameters, $V_{pd\sigma}$ and $V_{pd\pi}$:

$$V_{p_x d_{xy}1} = \frac{\sqrt{3}}{2\sqrt{2}}V_{pd\sigma}, \tag{14}$$

$$V_{p_x d_{yz}1} = -\frac{\sqrt{3}}{2\sqrt{2}}\theta V_{pd\sigma} + \frac{1}{\sqrt{2}}\theta V_{pd\pi}, \tag{15}$$

$$V_{p_x d_{xz}1} = -\frac{\sqrt{3}}{2\sqrt{2}}\theta V_{pd\sigma}, \tag{16}$$

$$V_{p_y d_{xz}1} = -\frac{\sqrt{3}}{2\sqrt{2}}\theta V_{pd\sigma} + \frac{1}{\sqrt{2}}\theta V_{pd\pi}, \tag{17}$$

$$V_{p_y d_{yz}1} = -\frac{\sqrt{3}}{2\sqrt{2}}\theta V_{pd\sigma}, \tag{18}$$

$$V_{p_y d_{xy}1} = \frac{\sqrt{3}}{2\sqrt{2}}V_{pd\sigma}, \tag{19}$$

$$V_{p_z d_{xz}1} = \frac{1}{\sqrt{2}}V_{pd\pi}, \tag{20}$$

$$V_{p_z d_{yz}1} = \frac{1}{\sqrt{2}}V_{pd\pi}, \tag{21}$$

$$V_{p_z d_{xy}1} = -\frac{\sqrt{3}}{2\sqrt{2}}\theta V_{pd\sigma} + \frac{1}{\sqrt{2}}\theta V_{pd\pi}, \tag{22}$$

where the $O(\theta^2)$ terms are neglected. Similarly, we obtain V_{a2A}:

$$V_{d_{xy}2p_x} = -V_{p_x d_{xy}1}, \tag{23}$$
$$V_{d_{yz}2p_x} = V_{p_x d_{yz}1}, \tag{24}$$
$$V_{d_{xz}2p_x} = V_{p_x d_{xz}1}, \tag{25}$$
$$V_{d_{xz}2p_y} = V_{p_y d_{xz}1}, \tag{26}$$
$$V_{d_{yz}2p_y} = V_{p_y d_{yz}1}, \tag{27}$$
$$V_{d_{xy}2p_y} = -V_{p_y d_{xy}1}, \tag{28}$$
$$V_{d_{xz}2p_z} = -V_{p_z d_{xz}1}, \tag{29}$$
$$V_{d_{yz}2p_z} = -V_{p_z d_{yz}1}, \tag{30}$$
$$V_{d_{xy}2p_z} = V_{p_z d_{xy}1}. \tag{31}$$

Combining Eqs. (14)–(31) with Eq. (13), we obtain the indirect hopping integrals within the $O(\theta^2)$ terms:

$$t_{d_{xy}2d_{xy}1}^{(\mathrm{indirect})} = -\frac{3V_{pd\sigma}^2}{4\Delta_{pd}}, \tag{32}$$

$$t_{d_{xz}2d_{xz}1}^{(\mathrm{indirect})} = -\frac{V_{pd\pi}^2}{2\Delta_{pd}}, \tag{33}$$

$$t_{d_{yz}2d_{yz}1}^{(\mathrm{indirect})} = t_{d_{xz}2d_{xz}1}^{(\mathrm{indirect})}, \tag{34}$$

$$t_{d_{xy}2d_{yz}1}^{(\mathrm{indirect})} = \theta\frac{3V_{pd\sigma}^2 - 2\sqrt{3}V_{pd\sigma}V_{pd\pi} + 2V_{pd\pi}^2}{4\Delta_{pd}}, \tag{35}$$

$$t_{d_{xy}2d_{xz}1}^{(\mathrm{indirect})} = t_{d_{xy}2d_{yz}1}^{(\mathrm{indirect})}, \tag{36}$$

$$t_{d_{yz}2d_{xz}1}^{(\mathrm{indirect})} = -\frac{V_{pd\pi}^2}{2\Delta_{pd}}, \tag{37}$$

$$t_{d_{xz}2d_{yz}1}^{(\mathrm{indirect})} = t_{d_{yz}2d_{xz}1}^{(\mathrm{indirect})}, \tag{38}$$

$$t_{d_{xz}2d_{xy}1}^{(\mathrm{indirect})} = -t_{d_{xy}2d_{xz}1}^{(\mathrm{indirect})}, \tag{39}$$

$$t_{d_{yz}2d_{xy}1}^{(\mathrm{indirect})} = -t_{d_{xy}2d_{yz}1}^{(\mathrm{indirect})}. \tag{40}$$

Those show that the deviation of the V-O-V angle from 180° leads to $t_{d_{xy}2d_{yz}1}^{(\mathrm{indirect})}$, $t_{d_{xy}2d_{xz}1}^{(\mathrm{indirect})}$, $t_{d_{yz}2d_{xy}1}^{(\mathrm{indirect})}$, and $t_{d_{xz}2d_{xy}1}^{(\mathrm{indirect})}$ even if the deviation angle θ is very small. The most important difference between those hopping integrals and the others, existing even for $\theta = 0°$, is the mirror symmetry about the xy plane including sublattices 1 and 2: those are odd-mirror, while the others are even-mirror. From a symmetrical point of view, the odd-mirror hopping integrals are permissible only without the inversion center because the mirror mixing occurs only without the inversion center. Although for not small θ, the deviation of the V-O-V angle affects not only $t_{d_{xy}2d_{yz}1}^{(\mathrm{indirect})}$, $t_{d_{xy}2d_{xz}1}^{(\mathrm{indirect})}$, $t_{d_{yz}2d_{xy}1}^{(\mathrm{indirect})}$, and $t_{d_{xz}2d_{xy}1}^{(\mathrm{indirect})}$ but also the other indirect ones, for the higher-order effects of θ the symmetry of the hopping integrals remains the same. Thus, the above derivation is sufficient to show the appearance of the odd-mirror hopping integrals due to the indirect hoppings through the O $2p$ orbitals under the deviation of the V-O-V angle from 180°.

By combining the direct hopping integrals and the indirect ones, the kinetic energy of the t_{2g}-orbital electrons for pyrochlore oxides can be described by three parameters of $\hat{H}_0$, i.e., t_1, t_2, and t_3, and one parameter of $\hat{H}_{\mathrm{odd}}$, i.e., t_{odd}. These parameters are related to the nearest-neighbor hopping integrals for the t_{2g}-orbital electrons. For example, those relations for the plane including sublattices 1 and 2 are given by

$$t_1 = t_{d_{xy}2d_{xy}1}^{(\mathrm{direct})} + t_{d_{xy}2d_{xy}1}^{(\mathrm{indirect})}, \tag{41}$$

$$t_2 = t_{d_{xz}2d_{xz}1}^{(\mathrm{direct})} + t_{d_{xz}2d_{xz}1}^{(\mathrm{indirect})} = t_{d_{yz}2d_{yz}1}^{(\mathrm{direct})} + t_{d_{yz}2d_{yz}1}^{(\mathrm{indirect})}, \tag{42}$$

$$t_3 = t_{d_{yz}2d_{xz}1}^{(\mathrm{direct})} + t_{d_{yz}2d_{xz}1}^{(\mathrm{indirect})} = t_{d_{xz}2d_{yz}1}^{(\mathrm{direct})} + t_{d_{xz}2d_{yz}1}^{(\mathrm{indirect})}, \tag{43}$$

$$t_{\mathrm{odd}} = t_{d_{xz}2d_{xy}1}^{(\mathrm{indirect})} = t_{d_{yz}2d_{xy}1}^{(\mathrm{indirect})} = -t_{d_{xy}2d_{xz}1}^{(\mathrm{indirect})} = -t_{d_{xy}2d_{yz}1}^{(\mathrm{indirect})}. \tag{44}$$

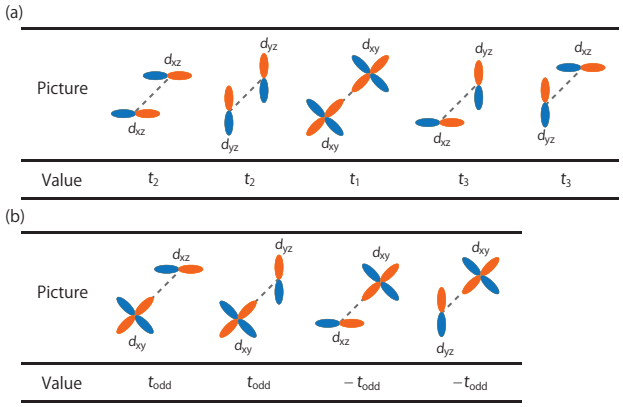

FIG. 3: Schematic pictures of (a) the even-mirror hoppings of $\hat{H}_0$ and (b) the odd-mirror hoppings of $\hat{H}_{\rm odd}$ for the nearest-neighbor V ions between sublatices 1 and 2 and the corresponding values. The color differences represent the sign differences of the wave function.

Those relations are more easily seen from Fig. 3. By choosing t_1, t_2, t_3, and $t_{\rm odd}$ appropriately, the Hamiltonian of Eq. (3) can describe the kinetic energy for any pyrochlore oxides as long as the main orbitals for low-energy excitations are the t_{2g} orbitals.

B. $\hat{H}_{\rm tri}$

The effect of the trigonal distortion on the t_{2g}-orbital electrons can be described by $\hat{H}_{\rm tri}$,

$$\hat{H}_{\rm tri} = -\frac{\Delta_{\rm tri}}{3}\sum_{\boldsymbol{i}}\sum_{a=d_{xz},d_{yz},d_{xy}}\sum_{b\neq a}\sum_{s=\uparrow,\downarrow}\hat{c}^{\dagger}_{\boldsymbol{i}as}\hat{c}_{\boldsymbol{i}bs}. \quad (45)$$

By diagonalizing $\hat{H}_{\rm tri}$, we rewrite $\hat{H}_{\rm tri}$ as

$$\hat{H}_{\rm tri} = -\frac{2\Delta_{\rm tri}}{3}\sum_{\boldsymbol{i}}\sum_{s=\uparrow,\downarrow}\hat{c}^{\dagger}_{\boldsymbol{i}a_{1g}s}\hat{c}_{\boldsymbol{i}a_{1g}s} + \frac{\Delta_{\rm tri}}{3}\sum_{\boldsymbol{i}}\sum_{s=\uparrow,\downarrow}(\hat{c}^{\dagger}_{\boldsymbol{i}e_g^+s}\hat{c}_{\boldsymbol{i}e_g^+s}+\hat{c}^{\dagger}_{\boldsymbol{i}e_g^-s}\hat{c}_{\boldsymbol{i}e_g^-s}), \quad (46)$$

where

$$\hat{c}^{\dagger}_{\boldsymbol{i}a_{1g}s} = \frac{1}{\sqrt{3}}(\hat{c}^{\dagger}_{\boldsymbol{i}d_{xz}s}+\hat{c}^{\dagger}_{\boldsymbol{i}d_{yz}s}+\hat{c}^{\dagger}_{\boldsymbol{i}d_{xy}s}), \quad (47)$$

$$\hat{c}^{\dagger}_{\boldsymbol{i}e_g^+s} = \frac{1}{\sqrt{3}}(\hat{c}^{\dagger}_{\boldsymbol{i}d_{xz}s}+\omega\hat{c}^{\dagger}_{\boldsymbol{i}d_{yz}s}+\omega^2\hat{c}^{\dagger}_{\boldsymbol{i}d_{xy}s}), \quad (48)$$

$$\hat{c}^{\dagger}_{\boldsymbol{i}e_g^-s} = \frac{1}{\sqrt{3}}(\hat{c}^{\dagger}_{\boldsymbol{i}d_{xz}s}+\omega^2\hat{c}^{\dagger}_{\boldsymbol{i}d_{yz}s}+\omega\hat{c}^{\dagger}_{\boldsymbol{i}d_{xy}s}), \quad (49)$$

and

$$\hat{c}_{\boldsymbol{i}a_{1g}s} = \frac{1}{\sqrt{3}}(\hat{c}_{\boldsymbol{i}d_{xz}s}+\hat{c}_{\boldsymbol{i}d_{yz}s}+\hat{c}_{\boldsymbol{i}d_{xy}s}), \quad (50)$$

$$\hat{c}_{\boldsymbol{i}e_g^+s} = \frac{1}{\sqrt{3}}(\hat{c}_{\boldsymbol{i}d_{xz}s}+\omega^2\hat{c}_{\boldsymbol{i}d_{yz}s}+\omega\hat{c}_{\boldsymbol{i}d_{xy}s}), \quad (51)$$

$$\hat{c}_{\boldsymbol{i}e_g^-s} = \frac{1}{\sqrt{3}}(\hat{c}_{\boldsymbol{i}d_{xz}s}+\omega\hat{c}_{\boldsymbol{i}d_{yz}s}+\omega^2\hat{c}_{\boldsymbol{i}d_{xy}s}), \quad (52)$$

with $\omega = e^{-\frac{2\pi}{3}i} = -\frac{1}{2}-i\frac{\sqrt{3}}{2}$ and $\omega^2 = e^{-\frac{4\pi}{3}i} = -\frac{1}{2}+i\frac{\sqrt{3}}{2}$. Thus, the effect of the trigonal distortion is splitting the energy level of the t_{2g}-orbital electron into the singlet a_{1g} orbital and the doublet e_g^+ and e_g^- orbitals, as shown in Fig. 1(b).

Since the a_{1g} orbital is the lower state for LiV_2O_4 and $Lu_2V_2O_7$ at low temperature, $\Delta_{\rm tri} > 0$ is realized for these pyrochlore vanadates. In principle, we can switch the lower state from the a_{1g} orbital to the e_g^+ and e_g^- orbitals by controlling the trigonal distortion.

If we express $\hat{H}_0$ and $\hat{H}_{\rm odd}$ in terms of the creation and annihilation operators for the a_{1g}, e_g^+, and e_g^- orbitals, we find the important difference between the even-mirror and the odd-mirror hopping integrals. Namely, the even-mirror hopping integrals for the t_{2g} orbitals are expressed as the intraorbital and the interorbital hopping integrals for the a_{1g}, e_g^+, and e_g^- orbitals, while the odd-mirror hopping integrals for the t_{2g} orbitals are expressed as the interorbital hopping integrals for the a_{1g}, e_g^+, and e_g^- orbitals. Those properties for the even-mirror and the odd-mirror hopping integrals are seen from, respectively, the intraorbital hopping integrals for the d_{xz} orbital between sublattice 2 at $\boldsymbol{i}=\boldsymbol{2}$ and subltattice 1 at $\boldsymbol{j}=\boldsymbol{1}$,

$$t_2\hat{c}^{\dagger}_{\boldsymbol{2}d_{xz}s}\hat{c}_{\boldsymbol{1}d_{xz}s} = \frac{t_2}{3}(\hat{c}^{\dagger}_{\boldsymbol{2}a_{1g}s}+\hat{c}^{\dagger}_{\boldsymbol{2}e_g^+s}+\hat{c}^{\dagger}_{\boldsymbol{2}e_g^+s})(\hat{c}_{\boldsymbol{1}a_{1g}s}+\hat{c}_{\boldsymbol{1}e_g^+s}+\hat{c}_{\boldsymbol{1}e_g^+s}), \quad (53)$$

and the odd-mirror hopping integrals between sublattice 2 at $\boldsymbol{i}=\boldsymbol{2}$ and subltattice 1 at $\boldsymbol{j}=\boldsymbol{1}$,

$$t_{\rm odd}(\hat{c}^{\dagger}_{\boldsymbol{2}d_{yz}s}\hat{c}_{\boldsymbol{1}d_{xy}s}+\hat{c}^{\dagger}_{\boldsymbol{2}d_{xz}s}\hat{c}_{\boldsymbol{1}d_{xy}s}-\hat{c}^{\dagger}_{\boldsymbol{2}d_{xy}s}\hat{c}_{\boldsymbol{1}d_{yz}s}-\hat{c}^{\dagger}_{\boldsymbol{2}d_{xy}s}\hat{c}_{\boldsymbol{1}d_{xz}s}) = t_{\rm odd}(\omega^2\hat{c}^{\dagger}_{\boldsymbol{2}a_{1g}s}\hat{c}_{\boldsymbol{1}e_g^+s}+\omega\hat{c}^{\dagger}_{\boldsymbol{2}a_{1g}s}\hat{c}_{\boldsymbol{1}e_g^-s}-\omega\hat{c}^{\dagger}_{\boldsymbol{2}e_g^+s}\hat{c}_{\boldsymbol{1}a_{1g}s} - \omega^2\hat{c}^{\dagger}_{\boldsymbol{2}e_g^-s}\hat{c}_{\boldsymbol{1}a_{1g}s}). \quad (54)$$

Understanding this difference is useful to understand the physical meaning of the finite contributions in the low-energy effective Hamiltonian (e.g., see Figs. 4 and 6).

C. $\hat{H}_{\rm int}$

$\hat{H}_{\rm int}$ is given by four multiorbital Hubbard interactions, U, U', $J_{\rm H}$, and J':

$$\begin{aligned}\hat{H}_{\rm int} =& U\sum_{\boldsymbol{i}}\sum_{a=d_{xz},d_{yz},d_{xy}}\hat{c}^\dagger_{\boldsymbol{i}a\uparrow}\hat{c}^\dagger_{\boldsymbol{i}a\downarrow}\hat{c}_{\boldsymbol{i}a\downarrow}\hat{c}_{\boldsymbol{i}a\uparrow}\\ &+U'\sum_{\boldsymbol{i}}\sum_{a=d_{xz},d_{yz},d_{xy}}\sum_{b>a}\sum_{s,s'=\uparrow,\downarrow}\hat{c}^\dagger_{\boldsymbol{i}as}\hat{c}^\dagger_{\boldsymbol{i}bs'}\hat{c}_{\boldsymbol{i}bs'}\hat{c}_{\boldsymbol{i}as}\\ &-J_{\rm H}\sum_{\boldsymbol{i}}\sum_{a=d_{xz},d_{yz},d_{xy}}\sum_{b>a}\sum_{s,s'=\uparrow,\downarrow}\hat{c}^\dagger_{\boldsymbol{i}as}\hat{c}^\dagger_{\boldsymbol{i}bs'}\hat{c}_{\boldsymbol{i}bs}\hat{c}_{\boldsymbol{i}as'}\\ &+J'\sum_{\boldsymbol{i}}\sum_{a=d_{xz},d_{yz},d_{xy}}\sum_{b\neq a}\hat{c}^\dagger_{\boldsymbol{i}a\uparrow}\hat{c}^\dagger_{\boldsymbol{i}a\downarrow}\hat{c}_{\boldsymbol{i}b\downarrow}\hat{c}_{\boldsymbol{i}b\uparrow},\end{aligned} \tag{55}$$

where $\sum_{b>a}$ represents the restricted summation, $\sum_{b>a}=\sum_{b=d_{yz},d_{xy}}$ or $\sum_{b=d_{xy}}$ or 0 for $a=d_{xz}$ or d_{yz} or d_{xy}, respectively. These four parameters reduce to two, U and $J_{\rm H}$, if we use $J'=J_{\rm H}$ and $U'=U-2J_{\rm H}$.

For the derivations of the low-energy effective Hamiltonian of the d^1 Mott insulator in Sec. III, we rewrite $\hat{H}_{\rm int}$ in terms of the irreducible representations of the d^2 states, where two electrons exist per site:

$$\hat{H}_{\rm int}=\sum_{\boldsymbol{i}}\sum_{\Gamma}\sum_{g_\Gamma}U_\Gamma|\boldsymbol{i};\Gamma,g_\Gamma\rangle\langle\boldsymbol{i};\Gamma,g_\Gamma|. \tag{56}$$

Here Γ represents the irreducible representations, g_Γ represents the degeneracy, U_Γ are given by

$$U_{A_1}=U+2J', \tag{57}$$
$$U_E=U-J', \tag{58}$$
$$U_{T_1}=U'-J_{\rm H}, \tag{59}$$
$$U_{T_2}=U'+J_{\rm H}, \tag{60}$$

and $|\boldsymbol{i};\Gamma,g_\Gamma\rangle$ are $|\boldsymbol{i};\Gamma,g_\Gamma\rangle=\hat{X}^\dagger_{\boldsymbol{i}\Gamma g_\Gamma}|0,0\rangle$ with

$$\hat{X}^\dagger_{\boldsymbol{i}A_1}=\frac{1}{\sqrt{3}}(\hat{c}^\dagger_{\boldsymbol{i}d_{xz}\uparrow}\hat{c}^\dagger_{\boldsymbol{i}d_{xz}\downarrow}+\hat{c}^\dagger_{\boldsymbol{i}d_{yz}\uparrow}\hat{c}^\dagger_{\boldsymbol{i}d_{yz}\downarrow}+\hat{c}^\dagger_{\boldsymbol{i}d_{xy}\uparrow}\hat{c}^\dagger_{\boldsymbol{i}d_{xy}\downarrow}), \tag{61}$$

$$\hat{X}^\dagger_{\boldsymbol{i}Eu}=\sqrt{\frac{2}{3}}(-\hat{c}^\dagger_{\boldsymbol{i}d_{xz}\uparrow}\hat{c}^\dagger_{\boldsymbol{i}d_{xz}\downarrow}+\frac{1}{2}\hat{c}^\dagger_{\boldsymbol{i}d_{yz}\uparrow}\hat{c}^\dagger_{\boldsymbol{i}d_{yz}\downarrow}+\frac{1}{2}\hat{c}^\dagger_{\boldsymbol{i}d_{xy}\uparrow}\hat{c}^\dagger_{\boldsymbol{i}d_{xy}\downarrow}), \tag{62}$$

$$\hat{X}^\dagger_{\boldsymbol{i}Ev}=\frac{1}{\sqrt{2}}(\hat{c}^\dagger_{\boldsymbol{i}d_{yz}\uparrow}\hat{c}^\dagger_{\boldsymbol{i}d_{yz}\downarrow}-\hat{c}^\dagger_{\boldsymbol{i}d_{xy}\uparrow}\hat{c}^\dagger_{\boldsymbol{i}d_{xy}\downarrow}), \tag{63}$$

$$\hat{X}^\dagger_{\boldsymbol{i}T_1\zeta_+}=\hat{c}^\dagger_{\boldsymbol{i}d_{xz}\uparrow}\hat{c}^\dagger_{\boldsymbol{i}d_{yz}\uparrow}, \tag{64}$$

$$\hat{X}^\dagger_{\boldsymbol{i}T_1\zeta_-}=\hat{c}^\dagger_{\boldsymbol{i}d_{xz}\downarrow}\hat{c}^\dagger_{\boldsymbol{i}d_{yz}\downarrow}, \tag{65}$$

$$\hat{X}^\dagger_{\boldsymbol{i}T_1\zeta_0}=\frac{1}{\sqrt{2}}(\hat{c}^\dagger_{\boldsymbol{i}d_{xz}\uparrow}\hat{c}^\dagger_{\boldsymbol{i}d_{yz}\downarrow}+\hat{c}^\dagger_{\boldsymbol{i}d_{xz}\downarrow}\hat{c}^\dagger_{\boldsymbol{i}d_{yz}\uparrow}), \tag{66}$$

$$\hat{X}^\dagger_{\boldsymbol{i}T_2\zeta_0}=\frac{1}{\sqrt{2}}(\hat{c}^\dagger_{\boldsymbol{i}d_{xz}\uparrow}\hat{c}^\dagger_{\boldsymbol{i}d_{yz}\downarrow}-\hat{c}^\dagger_{\boldsymbol{i}d_{xz}\downarrow}\hat{c}^\dagger_{\boldsymbol{i}d_{yz}\uparrow}), \tag{67}$$

$$\hat{X}^\dagger_{\boldsymbol{i}T_1\xi_+}=\hat{c}^\dagger_{\boldsymbol{i}d_{xz}\uparrow}\hat{c}^\dagger_{\boldsymbol{i}d_{xy}\uparrow}, \tag{68}$$

$$\hat{X}^\dagger_{\boldsymbol{i}T_1\xi_-}=\hat{c}^\dagger_{\boldsymbol{i}d_{xz}\downarrow}\hat{c}^\dagger_{\boldsymbol{i}d_{xy}\downarrow}, \tag{69}$$

$$\hat{X}^\dagger_{\boldsymbol{i}T_1\xi_0}=\frac{1}{\sqrt{2}}(\hat{c}^\dagger_{\boldsymbol{i}d_{xz}\uparrow}\hat{c}^\dagger_{\boldsymbol{i}d_{xy}\downarrow}+\hat{c}^\dagger_{\boldsymbol{i}d_{xz}\downarrow}\hat{c}^\dagger_{\boldsymbol{i}d_{xy}\uparrow}), \tag{70}$$

$$\hat{X}^\dagger_{\boldsymbol{i}T_2\xi_0}=\frac{1}{\sqrt{2}}(\hat{c}^\dagger_{\boldsymbol{i}d_{xz}\uparrow}\hat{c}^\dagger_{\boldsymbol{i}d_{xy}\downarrow}-\hat{c}^\dagger_{\boldsymbol{i}d_{xz}\downarrow}\hat{c}^\dagger_{\boldsymbol{i}d_{xy}\uparrow}), \tag{71}$$

$$\hat{X}^\dagger_{\boldsymbol{i}T_1\eta_+}=\hat{c}^\dagger_{\boldsymbol{i}d_{yz}\uparrow}\hat{c}^\dagger_{\boldsymbol{i}d_{xy}\uparrow}, \tag{72}$$

$$\hat{X}^\dagger_{\boldsymbol{i}T_1\eta_-}=\hat{c}^\dagger_{\boldsymbol{i}d_{yz}\downarrow}\hat{c}^\dagger_{\boldsymbol{i}d_{xy}\downarrow}, \tag{73}$$

$$\hat{X}^\dagger_{\boldsymbol{i}T_1\eta_0}=\frac{1}{\sqrt{2}}(\hat{c}^\dagger_{\boldsymbol{i}d_{yz}\uparrow}\hat{c}^\dagger_{\boldsymbol{i}d_{xy}\downarrow}+\hat{c}^\dagger_{\boldsymbol{i}d_{yz}\downarrow}\hat{c}^\dagger_{\boldsymbol{i}d_{xy}\uparrow}), \tag{74}$$

$$\hat{X}^\dagger_{\boldsymbol{i}T_2\eta_0}=\frac{1}{\sqrt{2}}(\hat{c}^\dagger_{\boldsymbol{i}d_{yz}\uparrow}\hat{c}^\dagger_{\boldsymbol{i}d_{xy}\downarrow}-\hat{c}^\dagger_{\boldsymbol{i}d_{yz}\downarrow}\hat{c}^\dagger_{\boldsymbol{i}d_{yx}\uparrow}). \tag{75}$$

D. $\hat{H}_{LS}$

$\hat{H}_{LS}$ is given by the atomic SOC, the so-called LS coupling, of the t_{2g}-orbital electrons:

$$\begin{aligned}\hat{H}_{\rm SOC}=&\frac{i\lambda_{LS}}{2}\sum_{\boldsymbol{i}}\sum_{s}{\rm sgn}(s)(\hat{c}^\dagger_{\boldsymbol{i}d_{yz}s}\hat{c}_{\boldsymbol{i}d_{xz}s}-\hat{c}^\dagger_{\boldsymbol{i}d_{xz}s}\hat{c}_{\boldsymbol{i}d_{yz}s})\\ &+\frac{i\lambda_{LS}}{2}\sum_{\boldsymbol{i}}\sum_{s}(\hat{c}^\dagger_{\boldsymbol{i}d_{xz}s}\hat{c}_{\boldsymbol{i}d_{xy}-s}-\hat{c}^\dagger_{\boldsymbol{i}d_{xy}-s}\hat{c}_{\boldsymbol{i}d_{xz}s})\\ &-\frac{\lambda_{LS}}{2}\sum_{\boldsymbol{i}}\sum_{s}{\rm sgn}(s)(\hat{c}^\dagger_{\boldsymbol{i}d_{yz}s}\hat{c}_{\boldsymbol{i}d_{xy}-s}-\hat{c}^\dagger_{\boldsymbol{i}d_{xy}s}\hat{c}_{\boldsymbol{i}d_{yz}-s}),\end{aligned} \tag{76}$$

with λ_{LS}, the coupling constant, ${\rm sgn}(\uparrow)=1$, ${\rm sgn}(\downarrow)=-1$, $-s=\downarrow$ for $s=\uparrow$, and $-s=\uparrow$ for $s=\downarrow$. The LS coupling is appropriate to take account of the SOC of electrons in solid. This is because the SOC of electrons arises from the relativistic effect near the nucleus, i.e. the correction to the nonrelativistic treatment is necessary only when an electron approaches the nucleus.

Actually, we can describe even the antisymmetric SOC for an inversion-symmetry-broken quasi-two-dimensional system near a surface or an interface by using $\hat{H}_{LS}$ and the appropriate hopping-integral terms such as $\hat{H}_{\rm odd}$[24,25]; this successful description holds not only for the effective single-orbital system, which is sufficiently described by a Rashba-type SOC[26], but also the t_{2g}-orbital system, which is not described by the Rashba-type SOC. The key to the successful description is the appropriate treatment of orbital degrees of freedom of the SOC and the kinetic energy.

$\hat{H}_{LS}$ causes not only the interorbital excitations for the t_{2g} orbitals but also the excitations between the a_{1g} orbital and the e_g^+ or e_g^- orbitals. The former is directly seen from Eq. (76), and the latter can be seen by rewriting Eq. (76) in terms of the creation and the annihilation operators of the a_{1g}, e_g^+, and e_g^- orbitals, Eqs. (47)–(52). The rewritten expression of Eq. (76) becomes

$$\begin{aligned}\hat{H}_{LS} =&\frac{i\lambda_{LS}}{6}\sum_{\boldsymbol{i}}\sum_{s}\mathrm{sgn}(s)\Big[(\omega^2-1)(\hat{c}^\dagger_{\boldsymbol{i}e_g^+s}\hat{c}_{\boldsymbol{i}a_{1g}s}-\hat{c}^\dagger_{\boldsymbol{i}a_{1g}s}\hat{c}_{\boldsymbol{i}e_g^-s})+(\omega-1)(\hat{c}^\dagger_{\boldsymbol{i}e_g^-s}\hat{c}_{\boldsymbol{i}a_{1g}s}-\hat{c}^\dagger_{\boldsymbol{i}a_{1g}s}\hat{c}_{\boldsymbol{i}e_g^+s})\Big]\\
&+\frac{i\lambda_{LS}}{6}\sum_{\boldsymbol{i}}\sum_{s}\Big[(1-\omega)(\hat{c}^\dagger_{\boldsymbol{i}e_g^+s}\hat{c}_{\boldsymbol{i}a_{1g}-s}-\hat{c}^\dagger_{\boldsymbol{i}a_{1g}s}\hat{c}_{\boldsymbol{i}e_g^--s})+(1-\omega^2)(\hat{c}^\dagger_{\boldsymbol{i}e_g^-s}\hat{c}_{\boldsymbol{i}a_{1g}-s}-\hat{c}^\dagger_{\boldsymbol{i}a_{1g}s}\hat{c}_{\boldsymbol{i}e_g^+-s})\Big]\\
&-\frac{\lambda_{LS}}{6}\sum_{\boldsymbol{i}}\sum_{s}\mathrm{sgn}(s)(\omega^2-\omega)(\hat{c}^\dagger_{\boldsymbol{i}e_g^+s}\hat{c}_{\boldsymbol{i}a_{1g}-s}+\hat{c}^\dagger_{\boldsymbol{i}a_{1g}s}\hat{c}_{\boldsymbol{i}e_g^+-s}-\hat{c}^\dagger_{\boldsymbol{i}e_g^-s}\hat{c}_{\boldsymbol{i}a_{1g}-s}-\hat{c}^\dagger_{\boldsymbol{i}a_{1g}s}\hat{c}_{\boldsymbol{i}e_g^-s})\\
&+(\text{others}).\end{aligned}\tag{77}$$

Here we have shown only the interorbital excitations between the a_{1g} orbital and the e_g^+ or e_g^- orbital explicitly, and the other terms have been written as (others). This is because those explicitly shown terms are sufficient for the derivation of the low-energy effective Hamiltonian, explained in Sec. III.

In addition, $\hat{H}_{LS}$ connects the different irreducible representations of the d^2 states for $\hat{H}_{\rm int}$. This can be shown by multiplying $\hat{H}_{LS}$ and $|\boldsymbol{i};\Gamma,g_\Gamma\rangle$; for example,

$$\begin{aligned}\hat{H}_{LS}|\boldsymbol{i};A_1\rangle =&-\frac{i\lambda_{LS}}{\sqrt{3}}(|\boldsymbol{i};T_1,\xi_+\rangle-|\boldsymbol{i};T_1,\xi_-\rangle)\\
&+\frac{\lambda_{LS}}{\sqrt{3}}(|\boldsymbol{i};T_1,\eta_+\rangle+|\boldsymbol{i};T_1,\eta_-\rangle)\\
&-\frac{i\lambda_{LS}\sqrt{2}}{\sqrt{3}}(|\boldsymbol{i};T_1,\zeta_0\rangle,\end{aligned}\tag{78}$$

$$\begin{aligned}\hat{H}_{LS}|\boldsymbol{i};E,u\rangle =&\frac{i\lambda_{LS}}{2\sqrt{6}}(|\boldsymbol{i};T_1,\xi_+\rangle-|\boldsymbol{i};T_1,\xi_-\rangle)\\
&+\frac{\lambda_{LS}}{\sqrt{6}}(|\boldsymbol{i};T_1,\eta_+\rangle+|\boldsymbol{i};T_1,\eta_-\rangle)\\
&+\frac{i\lambda_{LS}}{2\sqrt{3}}|\boldsymbol{i};T_1,\zeta_0\rangle,\end{aligned}\tag{79}$$

$$\begin{aligned}\hat{H}_{LS}|\boldsymbol{i};T_1,\eta_\pm\rangle =&\mp\frac{i\lambda_{LS}}{2}|\boldsymbol{i};T_1,\xi_\pm\rangle+\frac{\lambda_{LS}}{\sqrt{3}}|\boldsymbol{i};A_1\rangle\\
&+\frac{\lambda_{LS}}{\sqrt{6}}|\boldsymbol{i};E,u\rangle\\
&-\frac{i\lambda_{LS}}{2\sqrt{2}}(|\boldsymbol{i};T_1,\zeta_0\rangle\mp|\boldsymbol{i};T_2,\zeta_0\rangle),\end{aligned}\tag{80}$$

$$\begin{aligned}\hat{H}_{LS}|\boldsymbol{i};T_2,\eta_0\rangle =&-\frac{i\lambda_{LS}}{2}|\boldsymbol{i};T_1,\xi_0\rangle\\
&-\frac{i\lambda_{LS}}{2\sqrt{2}}(|\boldsymbol{i};T_1,\zeta_+\rangle-|\boldsymbol{i};T_1,\zeta_-\rangle).\end{aligned}\tag{81}$$

Thus, the LS coupling causes the excitations between the different d^2 multiplets; here we have assumed that $J_{\rm H}$ and J' are finite. As we will see in Sec. III B 2, this effect of the LS coupling leads to a new contribution to the low-energy effective Hamiltonian, which is missing in Moriya's microscopic theory[8].

Before going into the derivation of the low-energy effective Hamiltonian, we will see the important differences between the SOC expressed by the LS coupling and the SOC expressed by the spin-gauge potential. If we consider the SOC in a continuum, i.e., a system without lattice, the SOC can be expressed in terms of the 2×2 spin-gauge potential[27], $(A_{\rm S})_\alpha(r)=\sum_\beta A_\alpha^\beta(r)\sigma^\beta$ $(\alpha,\beta=x,y,z)$ with the Pauli matrices σ^β:

$$\begin{aligned}\hat{H}_{\rm SOC} =&\frac{e}{2m^2}(\boldsymbol{\nabla}V(r)\times\boldsymbol{s})\cdot\boldsymbol{p}\\
=&\frac{e}{2m^2}\boldsymbol{A}_{\rm S}(r)\cdot\boldsymbol{p}.\end{aligned}\tag{82}$$

This expression is also rewritten in terms of $A_\alpha^\beta(r)$ and the spin current[27]. In the spin-gauge-potential expression, the spin and the site dependence of the SOC is included, and the orbital dependence is neglected. Thus, the differences between this expression and the LS-coupling expression are about the site and the orbital dependence of the SOC. About the site dependence, only the onsite component of the SOC is sufficient to analyze the effects of the SOC in solids, i.e., the systems with lattice. This is because the relativistic effect on the electrons

in solids should be considered only near the nucleus, and because even an effectively off-site SOC, such as a single-orbital Rashba SOC[26], can be described by the SOC expressed by the LS coupling and the appropriate kinetic terms[24,25]. About the orbital dependence, its treatment in the spin-gauge-potential expression is insufficient for solids. This is because the orbital dependence arises from the orbital angular momentum, and because the orbital angular momentum plays significant roles in solids even with quenching of the orbital angular momentum; the examples of the significant roles are the anisotropies of the exchange interactions[8]. Actually, in Sec. III B 1, we show the important role of the orbital angular momentum in the intermediate states in the third-order perturbation terms. Since we focus on not continua but solids and a continuum cannot be connected to a solid due to a crucial difference in translational symmetry, the SOC can be more appropriately described by the LS coupling than by the spin-gauge potential. The reason why the expression of the spin-gauge potential becomes insufficient can be understood that we cannot choose any specific gauge about spins in the similar way to the magnetic field expressed by the vector potential and charge current, because the spins are nonconserved quantities due to the coupling of spin and orbital angular momenta; i.e., gauge invariance about spins does not exist.

III. LOW-ENERGY EFFECTIVE HAMILTONIAN

In this section, we derive the low-energy effective Hamiltonian for a d^1 Mott insulator in pyrochlore oxides by using the similar perturbation theory to Moriya's microscopic theory[8], and show the results of the rough estimations about the derived coefficients. In this derivation, we consider the d^1 case for our model, corresponding to case of $Lu_2V_2O_7$ for example, and use three assumptions. One is that the Hubbard interactions are so large that the system becomes the d^1 Mott insulator. Another is that the trigonal-distortion potential is larger than the terms of $\hat{H}_{\rm KE}$ and $\hat{H}_{LS}$. Due to those assumptions, the ground state of our model is the Mott insulator, in which one electron occupies the a_{1g} orbital at each site. Furthermore, we can use $\hat{H}_{\rm int}$ and $\hat{H}_{\rm tri}$ as the non-perturbative terms, and treat $\hat{H}_{\rm KE}$ and $\hat{H}_{LS}$ perturbatively. The other assumption is that U_Γ for all Γ are larger than $\Delta_{\rm tri}$. Due to this, we can more easily treat the effects of the non-perturbative terms because we can approximate $\frac{1}{-\frac{4\Delta_{\rm tri}}{3}-(\hat{H}_{\rm int}+\hat{H}_{\rm tri})}$ as $\frac{1}{-\hat{H}_{\rm int}}$. If such approximation is not used, the perturbation calculations become very difficult because the d^2 states diagonalizing $\hat{H}_{\rm int}$ are not equal to the d^2 states diagonalizing $\hat{H}_{\rm tri}$. If we represents those three assumptions as equations, the first one is $U, U' \gg |t_1|, |t_2|, |t_3|, |t_{\rm odd}|, \lambda_{LS}$, the second one is $\Delta_{\rm tri} \gg |t_1|, |t_2|, |t_3|, |t_{\rm odd}|, \lambda_{LS}$, and the third one is $U_\Gamma \gg \Delta_{\rm tri}$. If the inequality signs of these conditions hold, the low-energy effective Hamiltonian derived under the three assumptions remains the leading term. Thus, the derived low-energy effective Hamiltonian is a ubiquitous model for d^1 pyrochlore oxides with the strong electron-electron interaction, the possitive trigonal-distortion potential, and the weak SOC.

The derivations of the low-energy effective Hamiltonian and rough estimations are explained as follows. In Sec. III A, we calculate the second-order perturbation terms for our model by using $\hat{H}_{\rm KE}$ twice; the term by using $\hat{H}_{LS}$ twice is not shown because that does not give the exchange interactions but gives the interaction between the charge-density operators. This calculation is application of Anderson's theory[28] to our model. We also estimate the sign of the coefficient of the second-order terms as a function of $\frac{J_{\rm H}}{U}$ within the $O(\frac{J_{\rm H}}{U})$ terms in four limiting cases. In Sec. III B, we calculate the third-order perturbation terms for our model by using $\hat{H}_{\rm KE}$ twice and $\hat{H}_{LS}$ once; the terms by using $\hat{H}_{\rm KE}$ once and $\hat{H}_{LS}$ twice are zero. The finite terms come from three terms, $\hat{H}_{\rm 3rd}^{\rm KE-KE-}LS$, $\hat{H}_{\rm 3rd}^{LS-\rm KE-KE}$, and $\hat{H}_{\rm 3rd}^{\rm KE-}LS^{-\rm KE}$ (for each definition, see Sec. III B). As we will discuss in detail in Sec. IV, only $\hat{H}_{\rm 3rd}^{\rm KE-KE-}LS$ and $\hat{H}_{\rm 3rd}^{LS-\rm KE-KE}$ are taken into account in Moriya's theory[8], and the present theory can take account of not only the contribution included in Moriya's theory[8] but also the contribution neglected, $\hat{H}_{\rm 3rd}^{\rm KE-}LS^{-\rm KE}$. In addition to the derivations, within the $O(\frac{J_{\rm H}}{U})$ terms, we estimate the ratio of the coefficient of $\hat{H}_{\rm 3rd}^{\rm KE-KE-}LS + \hat{H}_{\rm 3rd}^{LS-\rm KE-KE}$ to that of the second-order terms as a function of the ratio of $t_{\rm odd}$ to $A = t_1 + t_2 + t_3$ or $B = t_2 + t_3$ the sum of the even-mirror hopping integrals in four cases, differing from the four cases for the second-order terms, and the ratio of the coefficient of $\hat{H}_{\rm 3rd}^{\rm KE-}LS^{-\rm KE}$ to that of $\hat{H}_{\rm 3rd}^{\rm KE-KE-}LS + \hat{H}_{\rm 3rd}^{LS-\rm KE-KE}$ as a function of $\frac{\Delta_{\rm tri}}{U}$ in the same four cases as those for the second-order terms. The former and latter results are shown in Secs. III B 1 and III B 2, respectively.

A. Second-order perturbation terms

Before the actual derivation of the contributions from the second-order perturbation terms, we explain what we should do. The second-order perturbation term, $\hat{H}_{\rm 2nd}$, is generally given by[29]

$$\hat{H}_{\rm 2nd} = \langle {\rm f}|\hat{H}_{\rm p}\frac{\hat{\phi}}{E_0 - \hat{H}_{\rm np}}\hat{H}_{\rm p}|{\rm i}\rangle \times |{\rm f}\rangle\langle {\rm i}|. \tag{83}$$

Here $\hat{H}_{\rm p}$ represents the perturbation terms, $\hat{H}_{\rm np}$ represents the non-perturbation terms, $|{\rm i}\rangle$ and $|{\rm f}\rangle$ represent the ground states only with $\hat{H}_{\rm np}$, E_0 is the ground-state energy, and $\hat{\phi}$ is the projection operator excluding the same-energy state[29]. In our case, Eq. (83) between sublattices 1 and 2 at $\boldsymbol{i} = \mathbf{1}$ and $\mathbf{2}$, respectively, becomes

$$(\hat{H}_{\rm 2nd})_{\mathbf{12}} = \sum_{s_1,s_2,s_3,s_4} \langle a_{1g}^{s_3}, a_{1g}^{s_4}|\hat{H}_{\rm KE}\frac{\hat{\phi}}{-\frac{4\Delta_{\rm tri}}{3} - (\hat{H}_{\rm int}+\hat{H}_{\rm tri})}\hat{H}_{\rm KE}|a_{1g}^{s_1}, a_{1g}^{s_2}\rangle \times |a_{1g}^{s_3}, a_{1g}^{s_4}\rangle\langle a_{1g}^{s_1}, a_{1g}^{s_2}|$$
$$\approx \sum_{\boldsymbol{i}=\mathbf{1},\mathbf{2}}\sum_{s_1,s_2,s_3,s_4}\sum_{\Gamma}\sum_{g_\Gamma}\frac{\langle a_{1g}^{s_3}, a_{1g}^{s_4}|\hat{H}_{\rm KE}|\boldsymbol{i};\Gamma,g_\Gamma\rangle\langle\boldsymbol{i};\Gamma,g_\Gamma|\hat{H}_{\rm KE}|a_{1g}^{s_1}, a_{1g}^{s_2}\rangle}{-E_\Gamma}|a_{1g}^{s_3}, a_{1g}^{s_4}\rangle\langle a_{1g}^{s_1}, a_{1g}^{s_2}|, \quad (84)$$

with $|a_{1g}^{s_1}, a_{1g}^{s_2}\rangle = \hat{c}^\dagger_{\mathbf{1}a_{1g}s_1}\hat{c}^\dagger_{\mathbf{2}a_{1g}s_2}|0,0\rangle$. Here we have neglected the second-order term for $\hat{H}_{LS}$ because that does not give the exchange interactions, as described. The operator part $|a_{1g}^{s_3}, a_{1g}^{s_4}\rangle\langle a_{1g}^{s_1}, a_{1g}^{s_2}|$ can be expressed in terms of the charge-density and the spin operators for the a_{1g} orbital, e.g. $|a_{1g}^{\uparrow}, a_{1g}^{\downarrow}\rangle\langle a_{1g}^{\uparrow}, a_{1g}^{\downarrow}| = (\frac{1}{2}\hat{n}_{\mathbf{1}} + \hat{s}^z_{\mathbf{1}})(\frac{1}{2}\hat{n}_{\mathbf{2}} - \hat{s}^z_{\mathbf{2}})$ or $|a_{1g}^{\uparrow}, a_{1g}^{\downarrow}\rangle\langle a_{1g}^{\downarrow}, a_{1g}^{\uparrow}| = \hat{s}^+_{\mathbf{1}}\hat{s}^-_{\mathbf{2}}$. Thus, what we should do is to express the right-hand side of Eq. (84) in terms of those operators, t_1, t_2, t_3, $t_{\rm odd}$, U, U', $J_{\rm H}$, and J'.

We can calculate the right-hand side of Eq. (84) for our model in the similar way for Ref. 17. As we will describe the detail of the calculation in Appendix A, we can express Eq. (84) as follows:

$$(\hat{H}_{\rm 2nd})_{\mathbf{12}} = J^{\rm AF}(\frac{1}{4}\hat{n}_{\mathbf{1}}\hat{n}_{\mathbf{2}} - \hat{\boldsymbol{s}}_{\mathbf{1}}\cdot\hat{\boldsymbol{s}}_{\mathbf{2}}) + J^{\rm FM}(\frac{3}{4}\hat{n}_{\mathbf{1}}\hat{n}_{\mathbf{2}} + \hat{\boldsymbol{s}}_{\mathbf{1}}\cdot\hat{\boldsymbol{s}}_{\mathbf{2}}), \quad (85)$$

with

$$J^{\rm AF} = -\frac{4}{27}\frac{(t_1+2t_2+2t_3)^2}{U+2J'} - \frac{8}{27}\frac{(t_1-t_2-t_3)^2+9t_{\rm odd}^2}{U-J'} - \frac{4}{9}\frac{(t_1+t_2+t_3)^2+2(t_2+t_3)^2+3t_{\rm odd}^2}{U'+J_{\rm H}}, \quad (86)$$

$$J^{\rm FM} = -\frac{4}{9}\frac{(t_1-t_2-t_3)^2+9t_{\rm odd}^2}{U'-J_{\rm H}}. \quad (87)$$

Some of the processes of the second-order perturbation are shown in Figs. 4(a) and 4(b). Thus, the second-order perturbation terms give the AF and the FM superexchange interactions. Since the superexchange interactions between sublattices 1 and 2 are isotropic about the spin operators, the superexchange interactions between the other two sublattices are the same except the sign changes of t_3 and $t_{\rm odd}$.

Before the derivations of the DM interaction, we see the relation between $J_{\rm H}$ and the sign of $J^{\rm FM} - J^{\rm AF}$ in a rough calculation in order to understand when the dominant superexchange interactions become FM or AF. In this rough calculation, we use simple relations of the Slater-Koster parameters[30] ($V_{dd\sigma} = -2V_{dd\pi}$, $V_{dd\delta} = 0$, and $V_{pd\sigma} = -2V_{pd\pi}$), and set $J' = J_{\rm H}$ and $U' = U - 2J_{\rm H}$; then, we analyze the sign of $J^{\rm FM} - J^{\rm AF}$ within the $O(\frac{J_{\rm H}}{U})$ terms in four limiting cases, (i) $|V_{dd\pi}| \gg |\frac{V_{pd\pi}^2}{\Delta_{pd}}|$, (ii) $|V_{dd\pi}| \ll |\frac{V_{pd\pi}^2}{\Delta_{pd}}|$, (iii) $V_{dd\pi} \sim -\frac{V_{pd\pi}^2}{\Delta_{pd}}$, and (iv) $V_{dd\pi} \sim \frac{V_{pd\pi}^2}{\Delta_{pd}}$. Those limiting cases are sufficient for qualitative analyses of the $J_{\rm H}$ dependence of $J^{\rm FM} - J^{\rm AF}$ because as results of the simple relations, the direct and the indirect hopping integrals can be expressed by $V_{dd\pi}$ and $\frac{V_{pd\pi}^2}{\Delta_{pd}}$, respectively, and because in combination with $J' = J_{\rm H}$ and $U' = U - 2J_{\rm H}$, $J^{\rm FM} - J^{\rm AF}$ can be expressed in terms of $V_{dd\pi}$, $\frac{V_{pd\pi}^2}{\Delta_{pd}}$, U, and $J_{\rm H}$. To estimate the order of critical $\frac{J_{\rm H}}{U}$ for the boundary between the AF and FM interactions in each limiting case, we assume that θ is so small that the terms of the odd-mirror hopping integrals are negligible; if we include the terms, the critical $J_{\rm H}/U$ becomes smaller because the terms assist the FM interactions [see Eq. (88)]. Setting $J' = J_{\rm H}$ and $U' = U - 2J_{\rm H}$ in Eqs. (86) and (87) and expanding $J^{\rm FM} - J^{\rm AF}$ in a power series about $\frac{J_{\rm H}}{U}$ within the $O(\frac{J_{\rm H}}{U})$ terms, we rewrite $J^{\rm FM} - J^{\rm AF}$ as

$$J^{\rm FM} - J^{\rm AF} = \frac{4}{9U}\{(A+B)^2 - 2(\frac{J_{\rm H}}{U})[(A-2B)^2 + 9t_{\rm odd}^2]\}, \quad (88)$$

with $A = t_1+t_2+t_3$ and $B = t_2+t_3$. Then, by neglecting the $t_{\rm odd}^2$ terms, using the simple relations of the Slater-Koster parameters and considering the leading terms of $J^{\rm FM} - J^{\rm AF}$ in each limiting case, the leading terms in cases (i), (ii), (iii), and (iv) are given by

$$J^{\rm FM} - J^{\rm AF} \sim \frac{1}{9U}V_{dd\pi}^2(1 - 50\frac{J_{\rm H}}{U}), \quad (89)$$

$$J^{\rm FM} - J^{\rm AF} \sim \frac{100}{9U}(\frac{V_{pd\pi}^2}{\Delta_{pd}})^2(1 - \frac{8}{25}\frac{J_{\rm H}}{U}), \quad (90)$$

$$J^{\rm FM} - J^{\rm AF} \sim \frac{121}{9U}V_{dd\pi}^2(1 - \frac{2}{121}\frac{J_{\rm H}}{U}), \quad (91)$$

and

$$J^{\rm FM} - J^{\rm AF} \sim \frac{9}{U}V_{dd\pi}^2(1 - 2\frac{J_{\rm H}}{U}), \quad (92)$$

respectively. Thus, the order of the critical $\frac{J_{\rm H}}{U}$ becomes $O(0.01)$ for case (i), $O(1)$ for case (ii), $O(10)$ for case (iii), and $O(0.1)$ for case (iv); those results are summarized in Fig. 5. Since case (iv) may be the most realistic situation as pyrochlore vanadates[4], the superexchange interactions for the d^1 Mott insulator in the pyrochlore vanadates are FM for a realistic value of $\frac{J_{\rm H}}{U}$.

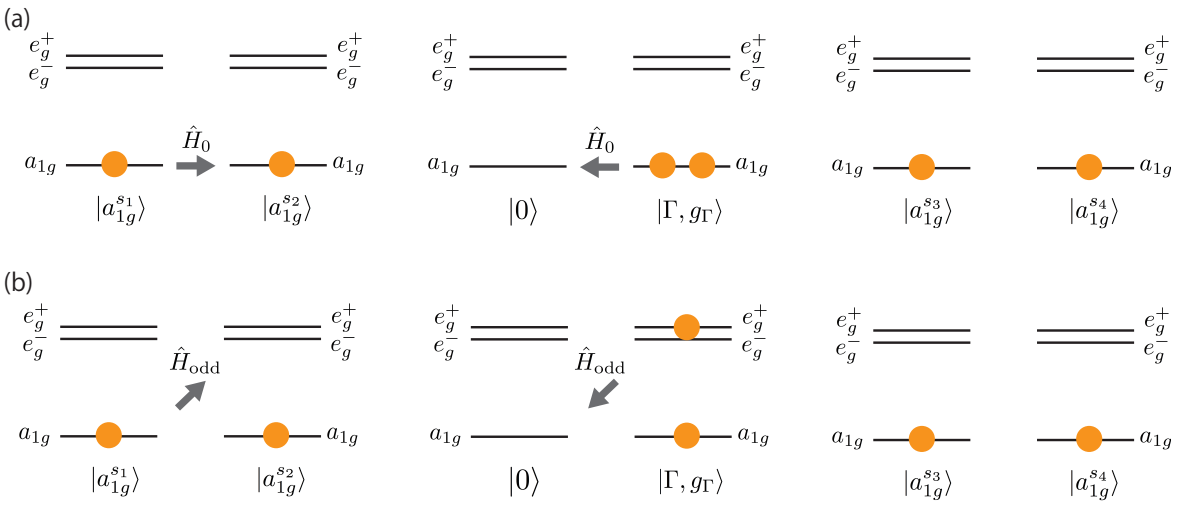

FIG. 4: Schematic pictures of examples of the processes of the second-order perturbation by (a) using $\hat{H}_0$ and (b) using $\hat{H}_{\rm odd}$. Yellow circles denote the electrons, and gray arrows denote the perturbations.

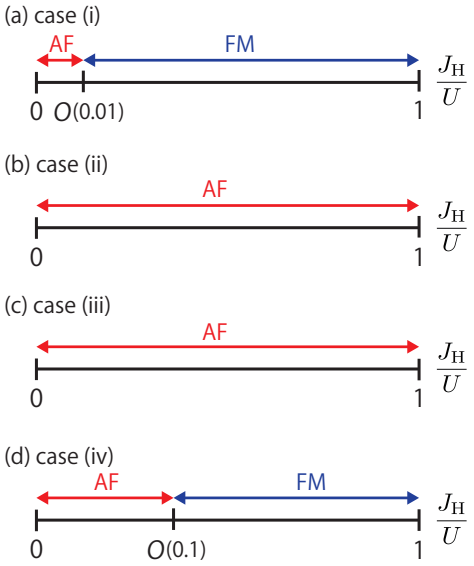

FIG. 5: Relation between $\frac{J_{\rm H}}{U}$ and the sign of $J^{\rm FM} - J^{\rm AF}$ in the four limiting cases without the $t_{\rm odd}^2$ terms within the $O(\frac{J_{\rm H}}{U})$ terms for $J' = J_{\rm H}$ and $U' = U - 2J_{\rm H}$. $J^{\rm FM} - J^{\rm AF}$ becomes AF or FM in the red-line region or the blue-line region, respectively. Since $J^{\rm FM} - J^{\rm AF}$ is expressed by the power series of $\frac{J_{\rm H}}{U}$, the results are meaningful only for $\frac{J_{\rm H}}{U} < 1$.

B. Third-order perturbation terms

As for the second-order perturbation terms, we start to prescribe what we should calculate for the third-order perturbation terms. The third-order perturbation terms for our model are given by

$$\begin{aligned}\hat{H}_{\rm 3rd} =& \hat{H}_{\rm 3rd}^{\rm KE-KE-\mathit{LS}} + \hat{H}_{\rm 3rd}^{\mathit{LS}-\rm KE-KE} + \hat{H}_{\rm 3rd}^{\rm KE-\mathit{LS}-KE} \\ =& \sum_{n_1,n_2} \frac{\langle \mathrm{f}|\hat{H}_{\rm KE}|n_1\rangle\langle n_1|\hat{\phi}\hat{H}_{\rm KE}|n_2\rangle\langle n_2|\hat{\phi}\hat{H}_{LS}|\mathrm{i}\rangle}{(E_0 - E_{n_1})(E_0 - E_{n_2})} |\mathrm{f}\rangle\langle \mathrm{i}| \\ &+ \sum_{n_1,n_2} \frac{\langle \mathrm{f}|\hat{H}_{LS}|n_2\rangle\langle n_2|\hat{\phi}\hat{H}_{\rm KE}|n_1\rangle\langle n_1|\hat{\phi}\hat{H}_{\rm KE}|\mathrm{i}\rangle}{(E_0 - E_{n_2})(E_0 - E_{n_1})} |\mathrm{f}\rangle\langle \mathrm{i}| \\ &+ \sum_{n_3,n_4} \frac{\langle \mathrm{f}|\hat{H}_{\rm KE}|n_3\rangle\langle n_3|\hat{\phi}\hat{H}_{LS}|n_4\rangle\langle n_4|\hat{\phi}\hat{H}_{\rm KE}|\mathrm{i}\rangle}{(E_0 - E_{n_3})(E_0 - E_{n_4})} |\mathrm{f}\rangle\langle \mathrm{i}|, \end{aligned} \tag{93}$$

where E_{n_i} represent the energies of $|n_i\rangle$; as described, the terms using $\hat{H}_{\rm KE}$ once and $\hat{H}_{LS}$ twice become zero. We will carry out the detailed calculation only for the third-order perturbation terms between sublattices 1 and 2, $(\hat{H}_{\rm 3rd})_{\mathbf{12}}$, because the other third-order perturbation terms can be derived from the result of $(\hat{H}_{\rm 3rd})_{\mathbf{12}}$ by permuting x, y, and z; for example, the terms between sublattices 1 and 3, $(\hat{H}_{\rm 3rd})_{\mathbf{13}}$, is obtained by replacing $(\hat{s}_{\mathbf{1}}^x, \hat{s}_{\mathbf{1}}^y, \hat{s}_{\mathbf{1}}^z)$ and $(\hat{s}_{\mathbf{2}}^x, \hat{s}_{\mathbf{2}}^y, \hat{s}_{\mathbf{2}}^z)$ in $(\hat{H}_{\rm 3rd})_{\mathbf{12}}$ by $(\hat{s}_{\mathbf{1}}^y, \hat{s}_{\mathbf{1}}^z, \hat{s}_{\mathbf{1}}^x)$ and $(\hat{s}_{\mathbf{3}}^y, \hat{s}_{\mathbf{3}}^z, \hat{s}_{\mathbf{3}}^x)$, respectively. The important differences among the three terms of $(\hat{H}_{\rm 3rd})_{\mathbf{12}}$ in Eq. (93) are about the intermediate states: in the first and the second term, $|n_1\rangle$ belongs to one of the d^2-d^0 or the d^0-d^2 states, such as $\hat{X}_{\mathbf{1}A_1}^\dagger|0,0\rangle$, and $|n_2\rangle$ belongs to one of the d^1-d^1 states for one a_{1g}-orbital state and one e_g^+- or e_g^--orbital state, such as $|a_{1g}^{s_1}, e_g^{+;s_2}\rangle = \hat{c}_{\mathbf{1}a_{1g}s_1}^\dagger \hat{c}_{\mathbf{2}e_g^+s_2}^\dagger |0,0\rangle$; in the third term, $|n_3\rangle$ and $|n_4\rangle$ belong to the d^2-d^0 or the d^0-d^2 states. Thus, in the first and the second term, $\hat{H}_{LS}$ causes the excitations between the a_{1g} orbital and the e_g^+ or e_g^- orbital; in the third term, $\hat{H}_{LS}$ causes the excitations between the different-energy irreducible representations of the d^2 states for $\hat{H}_{\rm int}$.

In the following, we will calculate each term of $(\hat{H}_{\rm 3rd})_{\mathbf{12}}$ in Eq. (93).

1. $\hat{H}_{3rd}^{KE-KE-LS}$ and $\hat{H}_{3rd}^{LS-KE-KE}$

We first calculate $\hat{H}_{\rm 3rd}^{\rm KE-KE-}{}^{LS}$ and $\hat{H}_{\rm 3rd}^{LS-\rm KE-KE}$ for two sites of sublattices 1 and 2. Since $\hat{H}_{\rm 3rd}^{LS-\rm KE-KE}$ is calculated from $\hat{H}_{\rm 3rd}^{LS-\rm KE-KE} = (\hat{H}_{\rm 3rd}^{\rm KE-KE-}{}^{LS})^\dagger$, we explain the derivation only for $\hat{H}_{\rm 3rd}^{\rm KE-KE-}{}^{LS}$. The derivation is divided into four steps because $\hat{H}_{\rm 3rd}^{\rm KE-KE-}{}^{LS}$ can be decomposed into the product of two operators:

$$\hat{H}_{\rm 3rd}^{\rm KE-KE-}{}^{LS} = \sum_{g_e=+,-} \hat{H}_{\rm exch}^{a_{1g}\text{-}e_g^{g_e}} \hat{H}_{\rm excit}^{e_g^{g_e}\text{-}a_{1g}}, \tag{94}$$

where

$$\hat{H}_{\rm exch}^{a_{1g}\text{-}e_g^{g_e}} = \sum_{n_1} \frac{\langle \mathrm{f}|\hat{H}_{\rm KE}|n_1\rangle\langle n_1|\hat{\phi}\hat{H}_{\rm KE}|n_2\rangle}{(E_0 - E_{n_1})} |\mathrm{f}\rangle\langle n_2|, \tag{95}$$

and

$$\hat{H}_{\rm excit}^{e_g^{g_e}\text{-}a_{1g}} = \frac{\langle n_2|\hat{\phi}\hat{H}_{\rm LS}|\mathrm{i}\rangle}{(E_0 - E_{n_2})} |n_2\rangle\langle \mathrm{i}|, \tag{96}$$

with $|\mathrm{i}\rangle = |a_{1g}^{s_1}, a_{1g}^{s_2}\rangle$, $|\mathrm{f}\rangle = |a_{1g}^{s_3}, a_{1g}^{s_4}\rangle$, $|n_2\rangle = |a_{1g}^{s_1}, e_g^{g_e;s_2'}\rangle$ or $|e_g^{g_e;s_1'}, a_{1g}^{s_2}\rangle$, and $|n_1\rangle = |\boldsymbol{i};\Gamma,g_\Gamma\rangle$. The first step is to derive $\hat{H}_{\rm exch}^{a_{1g}\text{-}e_g^{g_e}}$. This is similar for the derivation of the second-order perturbation terms. The second step is to derive $\hat{H}_{\rm excit}^{e_g^{g_e}\text{-}a_{1g}}$. This is the calculation of the finite matrix elements of $\hat{H}_{LS}$ for the excitations between the a_{1g} orbital and the e_g^+ or e_g^- orbital. The third step is to combine those two results by using Eq. (94). The fourth step is to combine the results for $\hat{H}_{\rm 3rd}^{\rm KE-KE-}{}^{LS}$ and $\hat{H}_{\rm 3rd}^{LS-\rm KE-KE}$.

We begin with the first step. In the similar way for the second-order perturbation terms, we can calculate $\hat{H}_{\rm exch}^{a_{1g}\text{-}e_g^{g_e}}$ for two sites of sublattices 1 and 2 for our model (for the details, see Appendix B):

$$\begin{aligned}
&(\hat{H}_{\rm exch}^{a_{1g}\text{-}e_g^{g_e}})_{\mathbf{12}} \\
=&\tilde{J}_{\rm S}^{\rm AF}\omega^{n(g_e)}[(\frac{1}{4}\hat{n}_{\mathbf{1}}\hat{o}_{\mathbf{2}}^{g_e} - \hat{\boldsymbol{s}}_{\mathbf{1}}\cdot\hat{\boldsymbol{so}}_{\mathbf{2}}^{g_e}) + (\frac{1}{4}\hat{o}_{\mathbf{1}}^{g_e}\hat{n}_{\mathbf{2}} - \hat{\boldsymbol{so}}_{\mathbf{1}}^{g_e}\cdot\hat{\boldsymbol{s}}_{\mathbf{2}})] + \tilde{J}_{\rm S}^{\rm FM}\omega^{n(g_e)}[(\frac{3}{4}\hat{n}_{\mathbf{1}}\hat{o}_{\mathbf{2}}^{g_e} + \hat{\boldsymbol{s}}_{\mathbf{1}}\cdot\hat{\boldsymbol{so}}_{\mathbf{2}}^{g_e}) + (\frac{3}{4}\hat{o}_{\mathbf{1}}^{g_e}\hat{n}_{\mathbf{2}} + \hat{\boldsymbol{so}}_{\mathbf{1}}^{g_e}\cdot\hat{\boldsymbol{s}}_{\mathbf{2}})] \\
&+ \tilde{J}_{\rm A}^{\rm AF}\omega^{n(g_e)}[(\frac{1}{4}\hat{n}_{\mathbf{1}}\hat{o}_{\mathbf{2}}^{g_e} - \hat{\boldsymbol{s}}_{\mathbf{1}}\cdot\hat{\boldsymbol{so}}_{\mathbf{2}}^{g_e}) - (\frac{1}{4}\hat{o}_{\mathbf{1}}^{g_e}\hat{n}_{\mathbf{2}} - \hat{\boldsymbol{so}}_{\mathbf{1}}^{g_e}\cdot\hat{\boldsymbol{s}}_{\mathbf{2}})] + \tilde{J}_{\rm A}^{\rm FM}\omega^{n(g_e)}[(\frac{3}{4}\hat{n}_{\mathbf{1}}\hat{o}_{\mathbf{2}}^{g_e} + \hat{\boldsymbol{s}}_{\mathbf{1}}\cdot\hat{\boldsymbol{so}}_{\mathbf{2}}^{g_e}) - (\frac{3}{4}\hat{o}_{\mathbf{1}}^{g_e}\hat{n}_{\mathbf{2}} + \hat{\boldsymbol{so}}_{\mathbf{1}}^{g_e}\cdot\hat{\boldsymbol{s}}_{\mathbf{2}})],
\end{aligned} \tag{97}$$

with

$$\hat{o}_{\boldsymbol{i}}^{g_e} = \sum_{s=\uparrow,\downarrow} \hat{c}_{\boldsymbol{i}a_{1g}s}^\dagger \hat{c}_{\boldsymbol{i}e_g^{g_e}s}, \tag{98}$$

$$\hat{\boldsymbol{so}}_{\boldsymbol{i}}^{g_e} = \frac{1}{2}\sum_{s,s'=\uparrow,\downarrow} \hat{c}_{\boldsymbol{i}a_{1g}s}^\dagger(\boldsymbol{\sigma})_{ss'}\hat{c}_{\boldsymbol{i}e_g^{g_e}s'}, \tag{99}$$

$$\begin{aligned}
\tilde{J}_{\rm S}^{\rm AF} =& -\frac{4}{27}\frac{(t_1+2t_2+2t_3)(t_1-t_2-t_3)}{U+2J'} \\
&- \frac{2}{27}\frac{(t_1-t_2-t_3)(4t_1+2t_2+2t_3)+9t_{\rm odd}^2}{U-J'} \\
&- \frac{1}{9}\frac{-4(t_2+t_3)^2+(t_1+t_2+t_3)^2-6t_{\rm odd}^2}{U'+J_{\rm H}},
\end{aligned} \tag{100}$$

$$\tilde{J}_{\rm S}^{\rm FM} = -\frac{1}{9}\frac{(t_1-t_2-t_3)^2}{U'-J_{\rm H}}, \tag{101}$$

$$\begin{aligned}
\tilde{J}_{\rm A}^{\rm AF} =& \frac{4}{9}\frac{(t_1+2t_2+2t_3)t_{\rm odd}}{U+2J'} + \frac{2}{9}\frac{(t_1-t_2-t_3)t_{\rm odd}}{U-J'} \\
&- \frac{1}{3}\frac{(t_1-3t_2-3t_3)t_{\rm odd}}{U'+J_{\rm H}},
\end{aligned} \tag{102}$$

$$\tilde{J}_{\rm A}^{\rm FM} = -\frac{(t_1+t_2+t_3)t_{\rm odd}}{U'-J_{\rm H}}, \tag{103}$$

$$\omega^{n(g_e)} = \begin{cases} \omega^2 & \text{for } g_e = + \\ \omega & \text{for } g_e = - \end{cases}. \tag{104}$$

Equation (97) shows three important properties of $\hat{H}_{\rm exch}^{a_{1g}\text{-}e_g^{g_e}}$. First, as in the case with the second-order perturbation terms, $\hat{H}_{\rm exch}^{a_{1g}\text{-}e_g^{g_e}}$ has the FM-type and the AF-type interactions. Second, in contrast to the second-order perturbation terms, $\hat{H}_{\rm exch}^{a_{1g}\text{-}e_g^{g_e}}$ includes the orbital-density operator, $\hat{o}_{\boldsymbol{i}}^{g_e}$, and the spin-orbital-combined operator, $\hat{\boldsymbol{so}}_{\boldsymbol{i}}^{g_e}$. The orbital-density operator or the spin-orbital-combined operator is essentially different from, respectively, the charge-density operator, $\hat{n}_{\boldsymbol{i}}$, or the spin operator, $\hat{\boldsymbol{s}}_{\boldsymbol{i}}$, because the charge-density and the spin operators should be defined for the product of the creation and annihilation operators of an electron for the same orbital; $\hat{n}_{\boldsymbol{i}}$ and $\hat{\boldsymbol{s}}_{\boldsymbol{i}}$ for the a_{1g}-orbital electrons are defined as

$$\hat{n}_{\boldsymbol{i}} = \sum_{s=\uparrow,\downarrow} \hat{c}_{\boldsymbol{i}a_{1g}s}^\dagger \hat{c}_{\boldsymbol{i}a_{1g}s}, \tag{105}$$

and

$$\hat{\boldsymbol{s}}_{\boldsymbol{i}} = \frac{1}{2}\sum_{s,s'=\uparrow,\downarrow} \hat{c}_{\boldsymbol{i}a_{1g}s}^\dagger(\boldsymbol{\sigma})_{ss'}\hat{c}_{\boldsymbol{i}a_{1g}s'}, \tag{106}$$

respectively. Due to this property, $\hat{H}_{\rm exch}^{a_{1g}\text{-}e_g^{g_e}}$ can not be

regarded as the simple superexchange interactions such as the second-order perturbation terms. Third, $\hat{H}_{\rm exch}^{a_{1g}\text{-}e_g^{g_e}}$ possesses not only the symmetric terms, proportional to $\tilde{J}_{\rm S}^{\rm AF}$ or $\tilde{J}_{\rm S}^{\rm FM}$, but also the antisymmetric terms, proportional to $\tilde{J}_{\rm A}^{\rm AF}$ or $\tilde{J}_{\rm A}^{\rm FM}$. Here the terms for $\tilde{J}_{\rm S}^{\rm AF}$ and $\tilde{J}_{\rm S}^{\rm FM}$ have been referred to as the symmetric terms because those are symmetric about site indices, **1** and **2**; the terms for $\tilde{J}_{\rm A}^{\rm AF}$ and $\tilde{J}_{\rm A}^{\rm FM}$, which are antisymmetric about the site indices, have been referred to as the antisymmetric terms.

In the second step, we calculate $\hat{H}_{\rm excit}^{e_g^{g_e}\text{-}a_{1g}}$ from Eq. (96) using Eq. (77). The calculated result is

$$
\begin{aligned}
\hat{H}_{\rm excit}^{e_g^{g_e}\text{-}a_{1g}} =& -\frac{\lambda_{LS}}{6\Delta_{\rm tri}}|a_{1g}^{\uparrow}, e_g^{g_e;\uparrow}\rangle\{i(\omega^{n(g_e)}-1)\langle a_{1g}^{\uparrow}, a_{1g}^{\uparrow}| + [i(1-\omega^{m(g_e)}) - (\omega^{n(g_e)}-\omega^{m(g_e)})]\langle a_{1g}^{\uparrow}, a_{1g}^{\downarrow}|\}\\
&-\frac{\lambda_{LS}}{6\Delta_{\rm tri}}|e_g^{g_e;\uparrow}, a_{1g}^{\uparrow}\rangle\{i(\omega^{n(g_e)}-1)\langle a_{1g}^{\uparrow}, a_{1g}^{\uparrow}| + [i(1-\omega^{m(g_e)}) - (\omega^{n(g_e)}-\omega^{m(g_e)})]\langle a_{1g}^{\downarrow}, a_{1g}^{\uparrow}|\}\\
&-\frac{\lambda_{LS}}{6\Delta_{\rm tri}}|a_{1g}^{\uparrow}, e_g^{g_e;\downarrow}\rangle\{[i(1-\omega^{m(g_e)}) + (\omega^{n(g_e)}-\omega^{m(g_e)})]\langle a_{1g}^{\uparrow}, a_{1g}^{\uparrow}| - i(\omega^{n(g_e)}-1)\langle a_{1g}^{\uparrow}, a_{1g}^{\downarrow}|\}\\
&-\frac{\lambda_{LS}}{6\Delta_{\rm tri}}|e_g^{g_e;\uparrow}, a_{1g}^{\downarrow}\rangle\{i(\omega^{n(g_e)}-1)\langle a_{1g}^{\uparrow}, a_{1g}^{\downarrow}| + [i(1-\omega^{m(g_e)}) - (\omega^{n(g_e)}-\omega^{m(g_e)})]\langle a_{1g}^{\downarrow}, a_{1g}^{\downarrow}|\}\\
&-\frac{\lambda_{LS}}{6\Delta_{\rm tri}}|a_{1g}^{\downarrow}, e_g^{g_e;\uparrow}\rangle\{i(\omega^{n(g_e)}-1)\langle a_{1g}^{\downarrow}, a_{1g}^{\uparrow}| + [i(1-\omega^{m(g_e)}) - (\omega^{n(g_e)}-\omega^{m(g_e)})]\langle a_{1g}^{\downarrow}, a_{1g}^{\downarrow}|\}\\
&-\frac{\lambda_{\rm LS}}{6\Delta_{\rm tri}}|e_g^{g_e;\downarrow}, a_{1g}^{\uparrow}\rangle\{[i(1-\omega^{m(g_e)}) + (\omega^{n(g_e)}-\omega^{m(g_e)})]\langle a_{1g}^{\uparrow}, a_{1g}^{\uparrow}| - i(\omega^{n(g_e)}-1)\langle a_{1g}^{\downarrow}, a_{1g}^{\uparrow}|\}\\
&-\frac{\lambda_{LS}}{6\Delta_{\rm tri}}|a_{1g}^{\downarrow}, e_g^{g_e;\downarrow}\rangle\{[i(1-\omega^{m(g_e)}) + (\omega^{n(g_e)}-\omega^{m(g_e)})]\langle a_{1g}^{\downarrow}, a_{1g}^{\uparrow}| - i(\omega^{n(g_e)}-1)\langle a_{1g}^{\downarrow}, a_{1g}^{\downarrow}|\}\\
&-\frac{\lambda_{LS}}{6\Delta_{\rm tri}}|e_g^{g_e;\downarrow}, a_{1g}^{\downarrow}\rangle\{[i(1-\omega^{m(g_e)}) + (\omega^{n(g_e)}-\omega^{m(g_e)})]\langle a_{1g}^{\uparrow}, a_{1g}^{\downarrow}| - i(\omega^{n(g_e)}-1)\langle a_{1g}^{\downarrow}, a_{1g}^{\downarrow}|\}, \qquad (107)
\end{aligned}
$$

with

$$
\omega^{m(g_e)} = \begin{cases} \omega & \text{for } g_e = + \\ \omega^2 & \text{for } g_e = - \end{cases}. \qquad (108)
$$

Equation (107) clearly shows that the LS coupling induces the excitations between the a_{1g} orbital and the e_g^+ or e_g^- orbital at one of the two sites in the terms of $\hat{H}_{\rm 3rd}^{\rm KE-KE-}{}^{LS}$. More precisely, the terms proportional to $i(\omega^{n(g_e)}-1)$ in Eq. (107) are induced by the z components of the LS coupling, i.e., the LS couplings between the d_{xz} and d_{yz} orbitals; the terms proportional to $i(1-\omega^{m(g_e)})$ are induced by the x components, i.e., the LS couplings between the d_{xz} and d_{xy} orbitals; the terms proportional to $(\omega^{n(g_e)}-\omega^{m(g_e)})$ are induced by the y components, i.e., the LS couplings between the d_{yz} and d_{xy} orbitals.

In the third step, by combining Eqs. (97) and (107) with Eq. (94), we obtain $(\hat{H}_{\rm 3rd}^{\rm KE-KE-}{}^{LS})_{\mathbf{12}}$:

$$
\begin{aligned}
(\hat{H}^{\mathrm{KE-KE}-LS}_{\mathrm{3rd}})_{\mathbf{12}} =& -\sum_{g_e=+,-}\frac{\lambda_{LS}}{6\Delta_{\mathrm{tri}}}i(\omega^{n(g_e)}-1)[2\tilde{J}^{\mathrm{FM}}_{\mathrm{S}}(\hat{n}_{\mathbf{1}}\hat{S}^z_{\mathbf{2}}+\hat{S}^z_{\mathbf{1}}\hat{n}_{\mathbf{2}})-(\tilde{J}^{\mathrm{FM}}_{\mathrm{A}}+\tilde{J}^{\mathrm{AF}}_{\mathrm{A}})(\hat{S}^z_{\mathbf{1}}\hat{n}_{\mathbf{2}}-\hat{n}_{\mathbf{1}}\hat{S}^z_{\mathbf{2}})]\\
&-\sum_{g_e=+,-}\frac{\lambda_{LS}}{3\Delta_{\mathrm{tri}}}(\omega^{n(g_e)}-1)(\tilde{J}^{\mathrm{FM}}_{\mathrm{A}}-\tilde{J}^{\mathrm{AF}}_{\mathrm{A}})(\hat{S}^x_{\mathbf{1}}\hat{S}^y_{\mathbf{2}}-\hat{S}^y_{\mathbf{1}}\hat{S}^x_{\mathbf{2}})\\
&-\sum_{g_e=+,-}\frac{\lambda_{LS}}{6\Delta_{\mathrm{tri}}}i(1-\omega^{m(g_e)})[2\tilde{J}^{\mathrm{FM}}_{\mathrm{S}}(\hat{n}_{\mathbf{1}}\hat{S}^x_{\mathbf{2}}+\hat{S}^x_{\mathbf{1}}\hat{n}_{\mathbf{2}})+(\tilde{J}^{\mathrm{FM}}_{\mathrm{A}}+\tilde{J}^{\mathrm{AF}}_{\mathrm{A}})(\hat{n}_{\mathbf{1}}\hat{S}^x_{\mathbf{2}}-\hat{S}^x_{\mathbf{1}}\hat{n}_{\mathbf{2}})]\\
&-\sum_{g_e=+,-}\frac{\lambda_{LS}}{3\Delta_{\mathrm{tri}}}(1-\omega^{m(g_e)})(\tilde{J}^{\mathrm{FM}}_{\mathrm{A}}-\tilde{J}^{\mathrm{AF}}_{\mathrm{A}})(\hat{S}^y_{\mathbf{1}}\hat{S}^z_{\mathbf{2}}-\hat{S}^z_{\mathbf{1}}\hat{S}^y_{\mathbf{2}})\\
&-\sum_{g_e=+,-}\frac{\lambda_{LS}}{6\Delta_{\mathrm{tri}}}i(\omega^{m(g_e)}-\omega^{n(g_e)})[2\tilde{J}^{\mathrm{FM}}_{\mathrm{S}}(\hat{n}_{\mathbf{1}}\hat{S}^y_{\mathbf{2}}+\hat{S}^y_{\mathbf{1}}\hat{n}_{\mathbf{2}})+(\tilde{J}^{\mathrm{FM}}_{\mathrm{A}}+\tilde{J}^{\mathrm{AF}}_{\mathrm{A}})(\hat{n}_{\mathbf{1}}\hat{S}^y_{\mathbf{2}}-\hat{S}^y_{\mathbf{1}}\hat{n}_{\mathbf{2}})]\\
&-\sum_{g_e=+,-}\frac{\lambda_{LS}}{3\Delta_{\mathrm{tri}}}(\omega^{m(g_e)}-\omega^{n(g_e)})(\tilde{J}^{\mathrm{FM}}_{\mathrm{A}}-\tilde{J}^{\mathrm{AF}}_{\mathrm{A}})(\hat{S}^z_{\mathbf{1}}\hat{S}^x_{\mathbf{2}}-\hat{S}^x_{\mathbf{1}}\hat{S}^z_{\mathbf{2}}), \qquad (109)
\end{aligned}
$$

where we have used the relations,

$$
2(\frac{1}{4}\hat{n}_{\mathbf{1}}\hat{o}^{g_e}_{\mathbf{2}}-\hat{\boldsymbol{s}}_{\mathbf{1}}\cdot\hat{\boldsymbol{s}}\hat{\boldsymbol{o}}^{g_e}_{\mathbf{2}})=|a^{\uparrow}_{1g},a^{\downarrow}_{1g}\rangle\langle a^{\uparrow}_{1g},e^{g_e;\downarrow}_{g}|-|a^{\uparrow}_{1g},a^{\downarrow}_{1g}\rangle\langle a^{\downarrow}_{1g},e^{g_e;\uparrow}_{g}|-|a^{\downarrow}_{1g},a^{\uparrow}_{1g}\rangle\langle a^{\uparrow}_{1g},e^{g_e;\downarrow}_{g}|+|a^{\downarrow}_{1g},a^{\uparrow}_{1g}\rangle\langle a^{\downarrow}_{1g},e^{g_e;\uparrow}_{g}|, \qquad (110)
$$

$$
2(\frac{1}{4}\hat{o}^{g_e}_{\mathbf{1}}\hat{n}_{\mathbf{2}}-\hat{\boldsymbol{s}}\hat{\boldsymbol{o}}^{g_e}_{\mathbf{1}}\cdot\hat{\boldsymbol{s}}_{\mathbf{2}})=|a^{\uparrow}_{1g},a^{\downarrow}_{1g}\rangle\langle e^{g_e;\uparrow}_{g},a^{\downarrow}_{1g}|-|a^{\uparrow}_{1g},a^{\downarrow}_{1g}\rangle\langle e^{g_e;\downarrow}_{g},a^{\uparrow}_{1g}|-|a^{\downarrow}_{1g},a^{\uparrow}_{1g}\rangle\langle e^{g_e;\uparrow}_{g},a^{\downarrow}_{1g}|+|a^{\downarrow}_{1g},a^{\uparrow}_{1g}\rangle\langle e^{g_e;\downarrow}_{g},a^{\uparrow}_{1g}|, \qquad (111)
$$

$$
\begin{aligned}
2(\frac{3}{4}\hat{n}_{\mathbf{1}}\hat{o}^{g_e}_{\mathbf{2}}+\hat{\boldsymbol{s}}_{\mathbf{1}}\cdot\hat{\boldsymbol{s}}\hat{\boldsymbol{o}}^{g_e}_{\mathbf{2}})=&\,2|a^{\uparrow}_{1g},a^{\uparrow}_{1g}\rangle\langle a^{\uparrow}_{1g},e^{g_e;\uparrow}_{g}|+2|a^{\downarrow}_{1g},a^{\downarrow}_{1g}\rangle\langle a^{\downarrow}_{1g},e^{g_e;\downarrow}_{g}|+|a^{\uparrow}_{1g},a^{\downarrow}_{1g}\rangle\langle a^{\uparrow}_{1g},e^{g_e;\downarrow}_{g}|+|a^{\uparrow}_{1g},a^{\downarrow}_{1g}\rangle\langle a^{\downarrow}_{1g},e^{g_e;\uparrow}_{g}|\\
&+|a^{\downarrow}_{1g},a^{\uparrow}_{1g}\rangle\langle a^{\uparrow}_{1g},e^{g_e;\downarrow}_{g}|+|a^{\downarrow}_{1g},a^{\uparrow}_{1g}\rangle\langle a^{\downarrow}_{1g},e^{g_e;\uparrow}_{g}|, \qquad (112)\\
2(\frac{3}{4}\hat{o}^{g_e}_{\mathbf{1}}\hat{n}_{\mathbf{2}}+\hat{\boldsymbol{s}}\hat{\boldsymbol{o}}^{g_e}_{\mathbf{1}}\cdot\hat{\boldsymbol{s}}_{\mathbf{2}})=&\,2|a^{\uparrow}_{1g},a^{\uparrow}_{1g}\rangle\langle e^{g_e;\uparrow}_{g},a^{\uparrow}_{1g}|+2|a^{\downarrow}_{1g},a^{\downarrow}_{1g}\rangle\langle e^{g_e;\downarrow}_{g},a^{\downarrow}_{1g}|+|a^{\uparrow}_{1g},a^{\downarrow}_{1g}\rangle\langle e^{g_e;\uparrow}_{g},a^{\downarrow}_{1g}|+|a^{\uparrow}_{1g},a^{\downarrow}_{1g}\rangle\langle e^{g_e;\downarrow}_{g},a^{\uparrow}_{1g}|\\
&+|a^{\downarrow}_{1g},a^{\uparrow}_{1g}\rangle\langle e^{g_e;\uparrow}_{g},a^{\downarrow}_{1g}|+|a^{\downarrow}_{1g},a^{\uparrow}_{1g}\rangle\langle e^{g_e;\downarrow}_{g},a^{\uparrow}_{1g}|. \qquad (113)
\end{aligned}
$$

Using the relations between each term of Eq. (107) and each component of the LS coupling, described below Eq. (108), we see from Eq. (109) that the z, x, and y components of the LS coupling lead to, respectively, the z, x, and y components of the DM interaction in Eq. (109).

Since $(\hat{H}^{LS-\mathrm{KE-KE}}_{\mathrm{3rd}})_{\mathbf{12}}$ is calculated from Eq. (109) by using the equality, $\hat{H}^{LS-\mathrm{KE-KE}}_{\mathrm{3rd}}=(\hat{H}^{\mathrm{KE-KE}-LS}_{\mathrm{3rd}})^{\dagger}$, we obtain $\hat{H}^{\mathrm{KE-KE}-LS}_{\mathrm{3rd}}+\hat{H}^{LS-\mathrm{KE-KE}}_{\mathrm{3rd}}$ after taking the summation about $g_e=+,-$ using Eqs. (104) and (108):

$$
\begin{aligned}
&(\hat{H}^{\mathrm{KE-KE}-LS}_{\mathrm{3rd}})_{\mathbf{12}}+(\hat{H}^{LS-\mathrm{KE-KE}}_{\mathrm{3rd}})_{\mathbf{12}}\\
&=-D(\hat{S}^y_{\mathbf{1}}\hat{S}^z_{\mathbf{2}}-\hat{S}^z_{\mathbf{1}}\hat{S}^y_{\mathbf{2}})+D(\hat{S}^z_{\mathbf{1}}\hat{S}^x_{\mathbf{2}}-\hat{S}^x_{\mathbf{1}}\hat{S}^z_{\mathbf{2}}), \qquad (114)
\end{aligned}
$$

with

$$
\begin{aligned}
D=&-\frac{2\lambda_{LS}}{\Delta_{\mathrm{tri}}}(\tilde{J}^{\mathrm{FM}}_{\mathrm{A}}-\tilde{J}^{\mathrm{AF}}_{\mathrm{A}})\\
=&\frac{2\lambda_{LS}t_{\mathrm{odd}}}{\Delta_{\mathrm{tri}}}[\frac{t_1+t_2+t_3}{U'-J_{\mathrm{H}}}-\frac{4}{9}\frac{t_1+2t_2+2t_3}{U+2J'}\\
&-\frac{2}{9}\frac{t_1-t_2-t_3}{U-J'}+\frac{1}{3}\frac{t_1-3t_2-3t_3}{U'+J_{\mathrm{H}}}]. \qquad (115)
\end{aligned}
$$

This antisymmetric exchange interaction is the DM interaction; as we will discuss in Sec. IV, the symmetry of the finite components is consistent with the phenomenological argument[9] based on Moriya's rule[8]. Examples of the finite contributions to $\hat{H}^{\mathrm{KE-KE}-LS}_{\mathrm{3rd}}$ and $\hat{H}^{LS-\mathrm{KE-KE}}_{\mathrm{3rd}}$ are schematically shown in Figs. 6(a) and 6(b), respectively.

Before turning to the derivation of $\hat{H}^{\mathrm{KE}-LS-\mathrm{KE}}_{\mathrm{3rd}}$, we

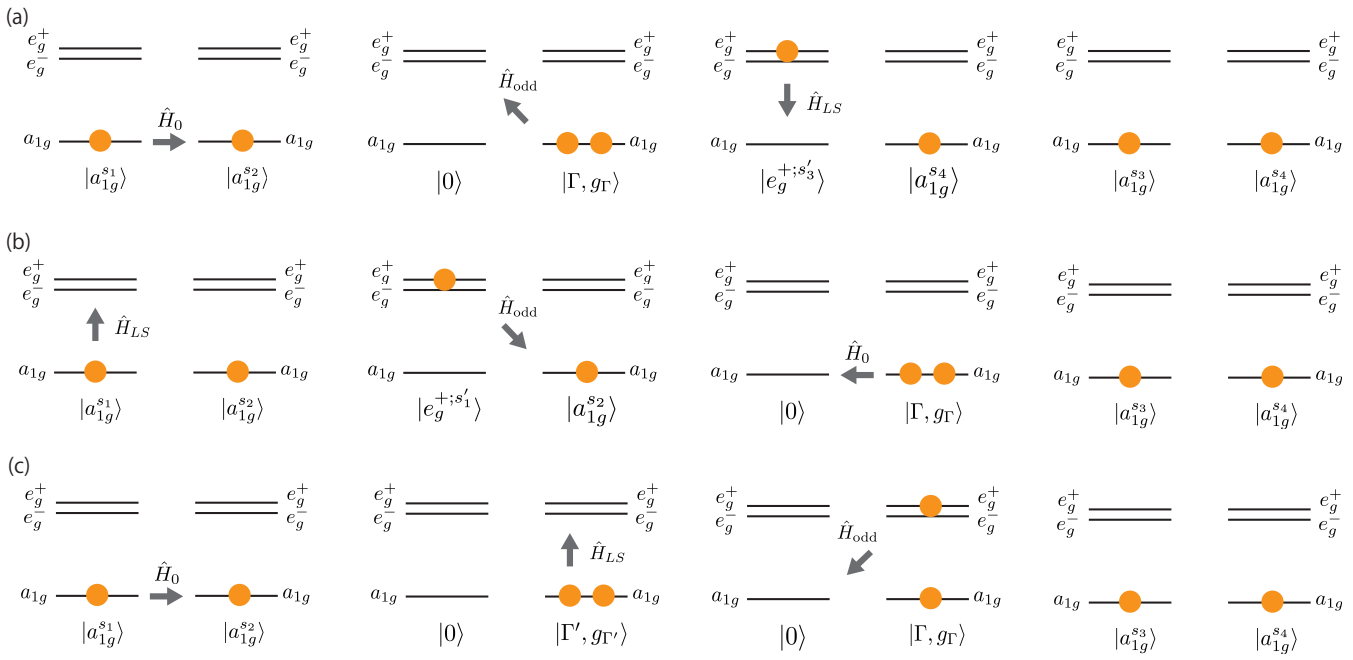

FIG. 6: Schematic pictures of examples of the processes of (a) $\hat{H}_{\rm 3rd}^{\rm KE-KE-}LS$, (b) $\hat{H}_{\rm 3rd}^{LS-\rm KE-KE}$, and (c) $\hat{H}_{\rm 3rd}^{\rm KE-}LS-\rm KE$. Yellow circles denote the electrons, and gray arrows denote the perturbations.

remark on several properties seen from the derived DM interaction because those are useful to understand the microscopic origin and ways to control it. First, from Eq. (109) and its dagger terms with Eqs. (100)–(103), we deduce that the DM interaction in $\hat{H}_{\rm 3rd}^{\rm KE-KE-}LS$ and $\hat{H}_{\rm 3rd}^{LS-\rm KE-KE}$ arises from the combination of the antisymmetric terms of $\hat{H}_{\rm exch}^{a_{1g}\text{-}e_g^{ge}}$ and the terms of $\hat{H}_{e_g^{ge}\text{-}a_{1g}}^{\rm exch}$. This highlights the importance of the mirror-mixing effect due to the combination of the antisymmetric kinetic exchange using the even-mirror hopping integrals and the odd-mirror hopping integral and the excitation of the LS coupling between the a_{1g} orbital and the e_g^+ or e_g^- orbital at one of the two sites. By a simpler argument, we can deduce from Eq. (114) the importance of the multiorbital properties and the mirror-mixing effect in the DM interaction, as we see in Appendix C. Then, the combination of the antisymmetric kinetic exchange and the excitation of the LS coupling is vital to obtain the DM interaction in the weak SOC because both give the antisymmetry between the two sites and because the combination of those antisymmetries is necessary to obtain the finite matrix elements of the perturbation terms between $|{\rm i}\rangle$ and $|{\rm f}\rangle$ in $\hat{H}_{\rm 3rd}^{\rm KE-KE-}LS$ and $\hat{H}_{\rm 3rd}^{LS-\rm KE-KE}$. In addition, the importance of the mirror-mixing effect shows the importance of the activation of the orbital angular momentum at one of the two sites in the intermediate states in the perturbation terms. This is because the orbital angular momentum is quenched in the non-perturbed states, i.e., $|{\rm i}\rangle$ and $|{\rm f}\rangle$, and because $\hat{H}_{\rm exch}^{a_{1g}\text{-}e_g^{ge}}$ and $\hat{H}_{e_g^{ge}\text{-}a_{1g}}^{\rm exch}$ cause the excitations between the a_{1g} orbital and the e_g^+ or e_g^- orbital at one of the two sites (see Fig. 6); in the degenerate e_g^+ and e_g^- orbitals, the orbital angular momentum is active, i.e., nonquenched. This important effect about the orbital angular momentum cannot be taken into account if the SOC is expressed in terms of the spin-gauge potential (see Sec. II D). As we will discuss in more detail in Sec. IV, the importance of the combination of the even-mirror and the odd-mirror hopping integral was not revealed in Moriya's microscopic theory[8] due to choosing a single parameter of the hopping integrals, and this microscopic origin of the DM interaction highlights the microscopic role of lack of the inversion center and the similarity to the microscopic origin in the strong SOC[17]. Then, Eq. (115) shows that the coefficient of the DM interaction in the weak SOC is given by the product of a ratio of λ_{LS} to $\Delta_{\rm tri}$ and the difference between the FM and the AF antisymmetric exchange interaction of $\hat{H}_{\rm exch}^{a_{1g}\text{-}e_g^{ge}}$. Thus, we can control the magnitude and sign of the DM interaction by tuning the relative strength of the FM and the AF exchange interactions (e.g., as a result of changing $J_{\rm H}$) or by changing the magnitude and sign of $t_{\rm odd}$ (as a result of changing the position of O ions). Those properties are clearly seen from Figs. 7(a)–(d); those figures are about the results of the rough estimation of $\frac{D}{J^{\rm FM}-J^{\rm AF}}$ within the $O(\frac{J_{\rm H}}{U})$ terms at $J'=J_{\rm H}$ and $U'=U-2J_{\rm H}$ in four cases, (a) $A \gg B$, (b) $A \ll B$, (c) $A \sim B$, and (d) $A \sim -B$, which are different from the four limiting cases considered in Sec. III A and III B 2. The detail of this estimation is described in Appendix D.

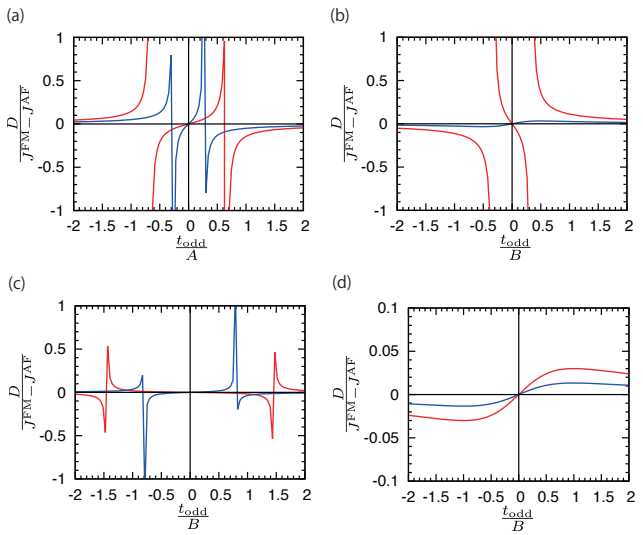

FIG. 7: $\frac{D}{J^{\rm FM}-J^{\rm AF}}$ as a function of $\frac{t_{\rm odd}}{A}$ in (a) $A \gg B$ or $\frac{t_{\rm odd}}{B}$ in (b) $A \ll B$ or (c) $A \sim B$ or (d) $A \sim -B$ for $\frac{J_{\rm H}}{U} = 0.1$ (red lines) and 0.3 (blue lines). $\frac{D}{J^{\rm FM}-J^{\rm AF}}$ were estimated by considering the $O(\frac{J_{\rm H}}{U})$ terms at $J' = J_{\rm H}$ and $U' = U - 2J_{\rm H}$ and setting $\lambda_{LS} = 0.03$ eV and $\Delta_{\rm tri} = 1$ eV in Eqs. (D3)–(D6). Those four cases are different from the four limiting cases considered in Figs. 5 and 8.

2. $\hat{H}^{KE-LS-KE}_{3rd}$

We turn to the calculation of $\hat{H}^{\rm KE-LS-KE}_{\rm 3rd}$ for two sites of sublattices 1 and 2. Since $\langle n_3|\hat{H}_{LS}|n_4\rangle$ in the third term of Eq. (93) represents the matrix elements between the different irreducible representations for the d^2 states for $\hat{H}_{\rm int}$, $\hat{H}^{\rm KE-LS-KE}_{\rm 3rd}$ can be obtained by using the results of $\langle n_4|\hat{H}_{\rm KE}|{\rm i}\rangle$ and $\langle {\rm f}|\hat{H}_{\rm KE}|n_3\rangle$ in the second-order perturbation terms with $\langle n_3|\hat{H}_{LS}|n_4\rangle$, such as Eqs. (78) and (79). By combining the contributions from every irreducible representation, $(\hat{H}^{\rm KE-LS-KE}_{\rm 3rd})_{\mathbf{12}}$ becomes

$$\begin{aligned}&(\hat{H}^{\rm KE-LS-KE}_{\rm 3rd})_{\mathbf{12}}\\ &= -D'(\hat{S}^y_{\mathbf{1}}\hat{S}^z_{\mathbf{2}} - \hat{S}^z_{\mathbf{1}}\hat{S}^y_{\mathbf{2}}) + D'(\hat{S}^z_{\mathbf{1}}\hat{S}^x_{\mathbf{2}} - \hat{S}^x_{\mathbf{1}}\hat{S}^z_{\mathbf{2}}),\end{aligned} \tag{116}$$

with

$$\begin{aligned}D' =& \frac{8\lambda_{LS}}{9}\frac{t_{\rm odd}(t_1+2t_2+2t_3)}{(U'-J_{\rm H})(U+2J')}\\ &+\frac{4\lambda_{LS}}{9}\frac{t_{\rm odd}(-t_1+4t_2+4t_3)}{(U'+J_{\rm H})(U'-J_{\rm H})}\\ &+\frac{8\lambda_{LS}}{9}\frac{t_{\rm odd}(t_1-t_2-t_3)}{9(U'-J_{\rm H})(U-J')},\end{aligned} \tag{117}$$

as derived in Appendix E. An example of the finite contributions to $(\hat{H}^{\rm KE-LS-KE}_{\rm 3rd})_{\mathbf{12}}$ is schematically shown in Fig. 6(c).

The DM interaction of Eq. (116) has the same symmetry as Eq. (114), and gives another contribution to the DM interaction between sublattices 1 and 2. As discussed in Sec. IV, this contribution was missing in Moriya's theory[8] because that considered a special case of the Hubbard interactions, i.e. $U' = U$ and $J_{\rm H} = J' = 0$, in which the irreducible representations merged into one state. However, the contribution using the inter-d^2-multiplet excitations is much smaller than the contribution using the interorbital excitations between the a_{1g} orbital and the e^+_g or e^-_g orbital in our considered case because $\frac{D'}{D} \sim O(\frac{\Delta_{\rm tri}}{U_\Gamma})$ is negligible in $U_\Gamma \gg \Delta_{\rm tri}$. If $\Delta_{\rm tri}$ becomes not much smaller than U_Γ, we should consider not only the contribution from $\hat{H}^{\rm KE-KE-LS}_{\rm 3rd} + \hat{H}^{LS-{\rm KE}-{\rm KE}}_{\rm 3rd}$ but also the contribution from $\hat{H}^{{\rm KE}-LS-{\rm KE}}_{\rm 3rd}$. More precise estimation of $\frac{D'}{D}$ can be carried out by the rough calculation which is similar to that for $J^{\rm FM} - J^{\rm AF}$ in Sec. III A. Namely, $\frac{D'}{D}$ within the $O(\frac{J_{\rm H}}{U})$ terms for $J' = J_{\rm H}$ and $U' = U - 2J_{\rm H}$ is given by

$$\frac{D'}{D} = \frac{\Delta_{\rm tri}}{U}\frac{(A+B)(1+2\frac{J_{\rm H}}{U})}{(A-2B)+6A\frac{J_{\rm H}}{U}}, \tag{118}$$

and the leading terms in the cases (a), (b), (c), and (d) considered in Sec. III A are, respectively,

$$\frac{D'}{D} = -\frac{\Delta_{\rm tri}}{U}\frac{1+2\frac{J_{\rm H}}{U}}{5+6\frac{J_{\rm H}}{U}}, \tag{119}$$

$$\frac{D'}{D} = \frac{5\Delta_{\rm tri}}{2U}\frac{1+2\frac{J_{\rm H}}{U}}{1+12\frac{J_{\rm H}}{U}}, \tag{120}$$

$$\frac{D'}{D} = -\frac{11\Delta_{\rm tri}}{U}\frac{1+2\frac{J_{\rm H}}{U}}{1-42\frac{J_{\rm H}}{U}}, \tag{121}$$

and

$$\frac{D'}{D} = \frac{\Delta_{\rm tri}}{U}\frac{1+2\frac{J_{\rm H}}{U}}{1+6\frac{J_{\rm H}}{U}}. \tag{122}$$

The leading terms depend on $\frac{\Delta_{\rm tri}}{U}$ in the way shown in Fig. 8. If we set $\Delta_{\rm tri} = 1$ eV and $U = 3$ eV (i.e., $\frac{\Delta_{\rm tri}}{U} \sim 0.3$) in Fig. 8(d), we find that the effect of the D' term is a small magnitude increase of the coefficient.

As the case with the remarks in Sec. III B 1, we deduce several properties of the derived DM interaction from Eqs. (116) and (117). First, the mirror-mixing effect is important even for this derived DM interaction because the numerators of D' consist of the products of the even-mirror and odd-mirror hopping integrals: the DM interaction using the inter-d^2-multiplet excitations can be also understood as the mirror-mixing effect. The similarity between $\hat{H}^{\rm KE-KE-LS}_{\rm 3rd} + \hat{H}^{LS-{\rm KE}-{\rm KE}}_{\rm 3rd}$ and $\hat{H}^{{\rm KE}-LS-{\rm KE}}_{\rm 3rd}$

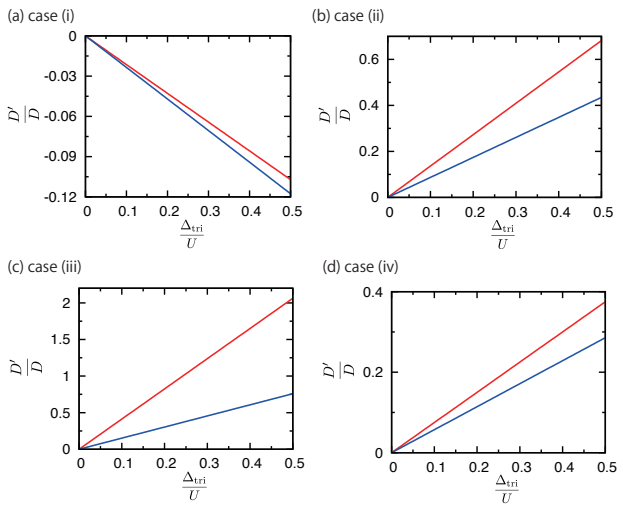

FIG. 8: $\frac{\Delta_{\rm tri}}{U}$ dependence of $\frac{D'}{D}$ in the four limiting cases considered in Fig. 5 for $\frac{J_{\rm H}}{U} = 0.1$ (red lines) and 0.3 (blue lines).

can be more easily seen by rewriting $\hat{H}_{\rm 3rd}^{\rm KE-LS-KE}$ as

$$\begin{aligned}&\hat{H}_{\rm 3rd}^{\rm KE-LS-KE}\\ =&\frac{1}{2}\sum_{n_3,n_4}\frac{\langle {\rm f}|\hat{H}_{\rm KE}|n_3\rangle\langle n_3|\hat{\phi}\hat{H}_{LS}|n_4\rangle\langle n_4|\hat{\phi}\hat{H}_{\rm KE}|{\rm i}\rangle}{(E_0-E_{n_3})(E_0-E_{n_4})}|{\rm f}\rangle\langle {\rm i}|\\ &+\frac{1}{2}\sum_{n_3,n_4}\frac{\langle {\rm f}|\hat{H}_{\rm KE}|n_4\rangle\langle n_4|\hat{\phi}\hat{H}_{LS}|n_3\rangle\langle n_3|\hat{\phi}\hat{H}_{\rm KE}|{\rm i}\rangle}{(E_0-E_{n_4})(E_0-E_{n_3})}|{\rm f}\rangle\langle {\rm i}|.\end{aligned} \tag{123}$$

Namely, the relation between the first and the second term of Eq. (123) is similar to the relation between $\hat{H}_{\rm 3rd}^{\rm KE-KE-LS}$ and $\hat{H}_{\rm 3rd}^{LS-\rm KE-KE}$. Then, the magnitude and sign of D' can be controlled by varying $J_{\rm H}$ or $t_{\rm odd}$.

IV. DISCUSSION

In this section, we discuss four points in order to clarify the meanings of our achievements. We first compare our results of the DM interaction derived microscopically with the result derived phenomenologically[9], and show what are new findings of our study. We next compare our microscopic theory formulated in this paper and Moriya's microscopic theory[8], and deduce the similarities and differences between them. Then, we argue the general applicability of our mechanism to the DM interaction in solids with the weak SOC. Finally, by comparison with the previous result in the strong SOC[17], we address the similarities and differences of the effects of the LS coupling on the low-energy effective Hamiltonian.

We begin with the comparison with the phenomenological theory[9] based on Moriya's rule[8]. By adopting Moriya's rule to the symmetry of the pyrochlore crystal, we can determine which terms of the DM interaction are permissible under the symmetry. Since the result of this phenomenological theory results from the symmetry, the finite components of the DM interaction obtained in the microscopic theory should be the same as that obtained in the phenomenological theory. Our results of the finite components are consistent with the results of the phenomenological theory[9]. Then, the phenomenological theory cannot reveal the microscopic origin of the DM interaction. On the other hand, our theory reveals the microscopic origin: the microscopic origin is the mirror-mixing effect by using the antisymmetric kinetic exchange of the even-mirror hopping and the odd-mirror hopping and the different-energy excitations of the LS coupling. In that effect, the role of the inversion-center lacking for each V-V bond is to induce the odd-mirror hopping integrals; since the even-mirror hopping integrals exist even with the inversion center, the inversion-center lacking is essential to obtain the antisymmetric kinetic exchange. Moreover, our theory can explain the microscopic reason why the mirror symmetry plays important roles in the phenomenological theory: the reason is that which plane's mirror symmetry is broken is linked with the kind of the permissible hopping integrals, which is important to discuss the mirror-mixing effect. Then, we highlight the close relation between the DM interaction and the sublattice structure for pyrochlore oxides: if we consider the DM interaction in pyrochlore oxides, we should simultaneously take account of the four-sublattice structure, shown in Fig. 1(a), because the inversion-center lacking causes not only the odd-mirror hopping but also the difference among four V ions in a tetrahedron as a result of the differences in the displacement of the O ion of each V-O-V bond. This relation provides an important restriction on the theory analyzing the DM interaction in pyrochlore oxides.

We next clarify the similarities and differences between the present theory and Moriya's microscopic theory[8]. In Moriya's microscopic theory, the SOC, one parameter of the kinetic term, and one parameter of the interaction term are considered, the third-order perturbation terms corresponding to $\hat{H}_{\rm 3rd}^{\rm KE-KE-LS}+\hat{H}_{\rm 3rd}^{LS-\rm KE-KE}$ in the present theory are calculated, and the DM interaction is obtained by using the excitations between the nondegenerate orbitals due to the SOC; the one parameter of the kinetic term corresponds to parameterizing all the hopping integrals by a single parameter; the one parameter of the interaction term is U, corresponding to a special case with $U'=U$ and $J_{\rm H}=J'=0$. On the other hand, the present theory includes the much more details of the kinetic term and interaction term, calculates not only $\hat{H}_{\rm 3rd}^{\rm KE-KE-LS}+\hat{H}_{\rm 3rd}^{LS-\rm KE-KE}$ but also another third-order perturbation term, $\hat{H}_{\rm 3rd}^{\rm KE-LS-KE}$, and obtains two different contributions to the DM interaction; the contribution from another is finite except the special case with $U'=U$ and $J_{\rm H}=J'=0$. Roughly speaking, by setting $t_1=t_2=t_3=t_{\rm odd}$, $U'=U$, and $J_{\rm H}=J'=0$, our theory reduces to Moriya's microscopic theory. Thus, the present theory reveals another contribution to the DM interaction within the third-order perturbation using the

kinetic term twice and the SOC once as a result of the difference in the four Hubbard interactions. In addition, the present theory clarifies the microscopic origin why the inversion-center lacking is necessary to obtain the DM interaction in the weak SOC as a result of the difference in the hopping integrals: the inversion-center lacking is necessary to get the antisymmetric kinetic exchange by using the even-mirror hopping once and the odd-mirror hopping once. Moreover, the present theory finds the dependence of the coefficients of the DM interaction on the typical four multiorbital Hubbard interactions. In particular, the simple relation between the difference between the FM and AF antisymmetric exchange interactions and the coefficient obtained for $\hat{H}_{\rm 3rd}^{\rm KE-KE-}{}^{LS} + \hat{H}_{\rm 3rd}^{LS-\rm KE-KE}$ is revealed. Those achievements develop our understanding of the physics of the DM interaction and suggest how to control it.

Then, we argue the general applicability of our mechanism. As we demonstrate below, our mechanism can explain the emergence of the DM interaction in any solids for the weak SOC if both the even-mirror hopping integral and the odd-mirror hopping integral are permissible and if there are at least two nondegenerate orbitals which are connected by the LS coupling. To demonstrate this generality, we consider two cases, a d-electron system in a cubic symmetry as a high-symmetry case and a t_{2g}-electron system in a tetragonal symmetry as a low-symmetry case. In the cubic symmetry, the five d orbitals split into the low-energy t_{2g} orbitals and the high-energy e_g orbitals. Whichever partially occupied cases [e.g., $(t_{2g})^1$ or $(t_{2g})^3$ configuration] we consider, the emergence of the DM interaction can be explained as the mirror-mixing effect if the odd-mirror hopping integral between the t_{2g} and e_g orbitals is permissible. This is because the LS coupling connects the t_{2g} and e_g orbitals and because the mirror-mixing effect using the even-mirror hopping integral, the odd-mirror hopping integral between the t_{2g} and e_g orbitals, and the LS coupling between them leads to the DM interaction, whose magnitude is either $O(\frac{t^{(\rm even)}t^{(\rm odd)}\lambda_{LS}}{U\Delta_{\rm cub}})$ for $U > \Delta_{\rm cub}$ or $O(\frac{t^{(\rm even)}t^{(\rm odd)}\lambda_{LS}}{\Delta_{\rm cub}^2})$ for $U < \Delta_{\rm cub}$, with $\Delta_{\rm cub}$, the energy difference between the t_{2g} and e_g orbitals. This cubic case for the $(t_{2g})^3$ configuration corresponds to, for example, $CdCr_2O_4$[12] at high temperature; here, we have neglected the effects of the trigonal-distortion potential because that may be small in AB_2O_4-type pyrochlore oxides (e.g., ~ 0.1 eV for LiV_2O_4[5]). Then, in the tetragonal symmetry, the t_{2g} orbitals, which are degenerate in the cubic symmetry, split into the d_{xy} orbital and the degenerate d_{xz} and d_{yz} orbitals. The degenerate d_{xz} and d_{yz} orbitals are low-energy for the c axis longer than the a and b axes (i.e., $c > a = b$), while the d_{xy} orbital is low-energy for the shorter c axis (i.e., $c < a = b$). The DM interaction in this tetragonal case can be also understood as the mirror-mixing effect using the even-mirror hopping integral, the odd-mirror hopping integral between the d_{xy} orbital and the d_{xz} or d_{yz} orbital, and the LS coupling between them; the magnitude is either $O(\frac{t^{(\rm even)}t^{(\rm odd)}\lambda_{LS}}{U\Delta_{\rm tetra}})$ for $U > \Delta_{\rm tetra}$ or $O(\frac{t^{(\rm even)}t^{(\rm odd)}\lambda_{LS}}{\Delta_{\rm tetra}^2})$ for $U < \Delta_{\rm tetra}$, with $\Delta_{\rm tetra}$, the energy difference between the d_{xy} orbital and the d_{xz} or d_{yz} orbital. For example, this tetragonal case with $c > a = b$ or $c < a = b$ for the $(t_{2g})^3$ configuration corresponds to $CdCr_2O_4$[12] at low temperature or $ZnCr_2O_4$[31] at low temperature, respectively (the effect of the trigonal distortion is neglected). Moreover, in the similar way, we can understand the DM interaction in not only other d-electron systems but also p-electron or f-electron systems with the weak SOC. This is because even for the DM interaction in those systems, the multiorbital properties and the mirror-mixing effect remain important to get the two characteristic properties of the DM interaction, as in the case of Appendix C. Thus, our mechanism provides the general mechanism for the DM interaction in solids with the weak SOC.

Finally, we compare the present theory in the weak-SOC system with the previous microscopic theory[17] in the strong-SOC system. In the latter theory, the low-energy effective model is derived for a d^5 Mott insulator in a quasi-two-dimensional t_{2g}-orbital Hubbard model on a square lattice with the inversion-symmetry breaking of an ab plane, and the DM interaction is obtained in the second-order perturbation, i.e., the same order of magnitude as the superexchange interaction. The difference between the two theories is the order of the perturbation to obtain the DM interaction. This can be understood as the difference in the effect of the LS coupling: in a weak-SOC system, the effect of the LS coupling can be treated perturbatively, and the orbital angular momentum is quenched; in a strong-SOC system, the nonperturbative treatment of the LS coupling becomes necessary, and the effects of the LS coupling causes the formation of the pseudospin as a result of the addition of the spin and orbital angular momenta. Namely, in the weak-SOC system, the combination of the second-order perturbation using the kinetic terms and the one-shot perturbation of the LS coupling is necessary to obtain the DM interaction because the LS coupling activates the orbital angular momentum, which is quenched in the nonperturbed states, at one of the two sites; in the strong-SOC system, the second-order perturbation using the kinetic terms is sufficient because the orbital angular momenta are not quenched and are not conserved quantities; i.e., the antisymmetry between the orbital angular momenta at two sites can be realized even in the nonperturbed states for the pseudospin. Then, the similarity between the two theories is the origin of the DM interaction, which is the mirror-mixing effect. Actually, the coefficient of the DM interaction in the strong-SOC system is given by the antisymmetric kinetic exchange, using the even-mirror hopping once and the odd-mirror hopping once; in the quasi-two-dimensional t_{2g}-orbital Hubbard model on a square lattice, the inversion-symmetry breaking of an ab plane induces the odd-mirror nearest-neighbor hoppings between the d_{yz} and d_{xy} orbitals along the x direction

and between the d_{xz} and d_{xy} orbitals along the y direction due to the similar mechanism for the present theory (to see the similarity, compare the derivations in Sec. II A and Sec. I of the Supplemental Material of Ref. 25). The above comparisons show that the DM interaction in solids can be understood in a unified way in the microscopic theories for the multiorbital models with the LS coupling, in which the effects of the inversion-center lacking are appropriately treated in the kinetic energy.

V. SUMMARY

In summary, we constructed the t_{2g}-orbital model for pyrochlore oxides, derived the low-energy effective Hamiltonian for the d^1 Mott insulator with the weak SOC, and clarified the microscopic origin of the DM interaction. First, the t_{2g}-orbital model was constructed by considering four terms: (1) the kinetic energy for not only the even-mirror hopping integrals, which exist even with the inversion center of each nearest-neighbor V-V bond, but also the odd-mirror hopping integrals, which appear only without the inversion center due to the indirect hoppings through the O-2p orbitals, (2) the trigonal-distortion potential, (3) the t_{2g}-orbital Hubbard interactions, and (4) the LS coupling. The main difference between this and the previous t_{2g}-orbital models[18–21] is the existence of the odd-mirror hopping integrals. Then, the low-energy effective Hamiltonian for the d^1 Mott insulator, where one electron occupied the a_{1g} orbital per site, was derived from the second-order perturbation terms using the nearest-neighbor hopping integrals twice and from the third-order perturbation terms using the hopping integrals twice and the LS coupling once; the second-order perturbation terms give the FM and the AF superexchange interactions, and the third-order perturbation terms give the DM interactions, whose symmetry is the same for the phenomenological theory[9]. The derived DM interactions consist of two contributions: one, corresponding to the DM interaction considered in Moriya's microscopic theory[8], arises from the combination of the interorbital excitation of the LS coupling between the a_{1g} and the e_g^+ or e_g^- orbital and the antisymmetric kinetic exchange, using the even-mirror hopping once and the odd-mirror hopping once; the other, which was missing in Moriya's microscopic theory[8], arises from the combination of the different-energy d^2-multiplet excitation of the LS coupling, and the even-mirror hopping integral and the odd-mirror hopping integral. The latter contribution appears except the special case with $U' = U$ and $J_{\rm H} = J' = 0$; the former contribution is dominant as long as the interactions are larger than the trigonal-distortion potential. The coefficients of those contributions revealed not only the importance of the mirror-mixing effect, but also the methods to control the DM interaction. One method is to tune the magnitude and sign of the odd-mirror hopping integral by changing the positions of the O ions; another is to tune the AF and the FM interactions by changing the t_{2g}-orbital Hubbard interactions.

Those achievements develop our understanding of the DM interaction in the weak SOC. In addition, our results showed the restriction on the theories studying the DM interaction in pyrochlore oxides: for such study, we should appropriately treat the four-sublattice structure of the V ions. Moreover, since we can apply the present theory to other multiorbital systems with the weak SOC, the present theory provides the general formalism to study the DM interaction in solids with the weak SOC.

Acknowledgments

I thank H. Tsunetsugu for pointing out that the essential symmetry in discussing the hopping integral under the inversion-center lacking is the mirror symmetry, and indicating the additional analyses about the sign of $J^{\rm FM} - J^{\rm AF}$, $\frac{D}{J^{\rm FM}-J^{\rm AF}}$, and $\frac{D'}{D}$. I also thank K. Riedl for useful discussions about Ref. 11.

Appendix A: Derivation of Eq. (85)

In this appendix, we derive Eq. (85) from Eq. (84) for our model. Equation (85) is derived by calculating the contribution from each $|\boldsymbol{i};\Gamma,g_\Gamma\rangle$ in Eq. (84), and the calculation from each contribution is similar to the calculation for a single-orbital system[28]. First, the contribution from $|\boldsymbol{i};\Gamma,g_\Gamma\rangle = |\boldsymbol{i};A_1\rangle$ becomes

$$-\frac{4}{27}\frac{(t_1+2t_2+2t_3)^2}{U+2J'}(\frac{1}{4}\hat{n}_{\boldsymbol{1}}\hat{n}_{\boldsymbol{2}} - \hat{\boldsymbol{s}}_{\boldsymbol{1}}\cdot\hat{\boldsymbol{s}}_{\boldsymbol{2}}). \tag{A1}$$

In this calculation, we first calculated the finite terms of $\langle \boldsymbol{i};A_1|\hat{H}_0+\hat{H}_{\rm odd}|a_{1g}^{s_1},a_{1g}^{s_2}\rangle$ for $\boldsymbol{i}=\boldsymbol{1},\boldsymbol{2}$ and $s_1,s_2=\uparrow,\downarrow$, and then expressed the contribution by using the finite matrix elements, $E_{A_1} = U+2J'$, and the corresponding operator part $|a_{1g}^{s_3},a_{1g}^{s_4}\rangle\langle a_{1g}^{s_1},a_{1g}^{s_2}|$. By the similar calculations, we obtain the contributions from the other $|\boldsymbol{i};\Gamma,g_\Gamma\rangle$: the contributions from $|\boldsymbol{i};\Gamma,g_\Gamma\rangle = |\boldsymbol{i};E,u\rangle$, $|\boldsymbol{i};E,v\rangle$, $|\boldsymbol{i};T_1,\xi_\pm\rangle$, $|\boldsymbol{i};T_1,\eta_\pm\rangle$, $|\boldsymbol{i};T_2,\zeta_0\rangle$, $|\boldsymbol{i};T_1,\xi_0\rangle$, $|\boldsymbol{i};T_2,\xi_0\rangle$, $|\boldsymbol{i};T_1,\eta_0\rangle$, and $|\boldsymbol{i};T_2,\eta_0\rangle$ are, respectively,

$$-\frac{2}{27}\frac{(t_1-t_2-t_3)^2+9t_{\rm odd}^2}{U-J'}(\frac{1}{4}\hat{n}_{\boldsymbol{1}}\hat{n}_{\boldsymbol{2}} - \hat{\boldsymbol{s}}_{\boldsymbol{1}}\cdot\hat{\boldsymbol{s}}_{\boldsymbol{2}}), \tag{A2}$$

$$-\frac{2}{9}\frac{(t_1-t_2-t_3)^2+9t_{\rm odd}^2}{U-J'}(\frac{1}{4}\hat{n}_{\boldsymbol{1}}\hat{n}_{\boldsymbol{2}} - \hat{\boldsymbol{s}}_{\boldsymbol{1}}\cdot\hat{\boldsymbol{s}}_{\boldsymbol{2}}), \tag{A3}$$

$$-\frac{2}{9}\frac{(t_1-t_2-t_3)^2+9t_{\rm odd}^2}{U'-J_{\rm H}}(\frac{1}{2}\hat{n}_{\boldsymbol{1}}\pm\hat{s}_{\boldsymbol{1}}^z)(\frac{1}{2}\hat{n}_{\boldsymbol{2}}\pm\hat{s}_{\boldsymbol{2}}^z), \tag{A4}$$

$$-\frac{2}{9}\frac{(t_1-t_2-t_3)^2+9t_{\rm odd}^2}{U'-J_{\rm H}}(\frac{1}{2}\hat{n}_{\boldsymbol{1}}\pm\hat{s}_{\boldsymbol{1}}^z)(\frac{1}{2}\hat{n}_{\boldsymbol{2}}\pm\hat{s}_{\boldsymbol{2}}^z), \tag{A5}$$

$$-\frac{8}{9}\frac{(t_2+t_3)^2+t_{\rm odd}^2}{U'+J_{\rm H}}(\frac{1}{4}\hat{n}_{\boldsymbol{1}}\hat{n}_{\boldsymbol{2}} - \hat{\boldsymbol{s}}_{\boldsymbol{1}}\cdot\hat{\boldsymbol{s}}_{\boldsymbol{2}}), \tag{A6}$$

$$-\frac{2}{9}\frac{(t_1-t_2-t_3)^2+9t_{\rm odd}^2}{U'-J_{\rm H}}(\frac{1}{4}\hat{n}_{\mathbf{1}}\hat{n}_{\mathbf{2}}-2\hat{s}_{\mathbf{1}}^z\hat{s}_{\mathbf{2}}^z+\hat{\boldsymbol{s}}_{\mathbf{1}}\cdot\hat{\boldsymbol{s}}_{\mathbf{2}}), \tag{A7}$$

$$-\frac{2}{9}\frac{(t_1+t_2+t_3)^2+t_{\rm odd}^2}{U'+J_{\rm H}}(\frac{1}{4}\hat{n}_{\mathbf{1}}\hat{n}_{\mathbf{2}}-\hat{\boldsymbol{s}}_{\mathbf{1}}\cdot\hat{\boldsymbol{s}}_{\mathbf{2}}), \tag{A8}$$

$$-\frac{2}{9}\frac{(t_1-t_2-t_3)^2+9t_{\rm odd}^2}{U'-J_{\rm H}}(\frac{1}{4}\hat{n}_{\mathbf{1}}\hat{n}_{\mathbf{2}}-2\hat{s}_{\mathbf{1}}^z\hat{s}_{\mathbf{2}}^z+\hat{\boldsymbol{s}}_{\mathbf{1}}\cdot\hat{\boldsymbol{s}}_{\mathbf{2}}), \tag{A9}$$

and

$$-\frac{2}{9}\frac{(t_1+t_2+t_3)^2+t_{\rm odd}^2}{U'+J_{\rm H}}(\frac{1}{4}\hat{n}_{\mathbf{1}}\hat{n}_{\mathbf{2}}-\hat{\boldsymbol{s}}_{\mathbf{1}}\cdot\hat{\boldsymbol{s}}_{\mathbf{2}}), \tag{A10}$$

and the contributions from $|\boldsymbol{i};\Gamma,g_\Gamma\rangle = |\boldsymbol{i};T_1,\zeta_\pm\rangle$, $|\boldsymbol{i};T_1,\zeta_0\rangle$ are zero for $(\hat{H}_{\rm 2nd})_{\mathbf{12}}$. Combining the contributions from all $|\boldsymbol{i};\Gamma,g_\Gamma\rangle$ for $\boldsymbol{i}=\mathbf{1},\mathbf{2}$ with Eq. (84), we obtain Eq. (85) with Eqs. (86) and (87).

Appendix B: Derivation of Eq. (97)

In this appendix, we derive Eq. (97). This derivation is similar to the derivation of Eq. (85), described in Appendix A, because Eq. (95) can be rewritten as

$$(\hat{H}_{\rm exch}^{a_{1g}\text{-}e_g^{g_e}})_{\mathbf{12}} \approx \sum_{\boldsymbol{i}=\mathbf{1},\mathbf{2}}\sum_{\Gamma}\sum_{g_\Gamma}\sum_{n_2}\sum_{s_3,s_4} \times \frac{\langle a_{1g}^{s_3},a_{1g}^{s_4}|\hat{H}_{\rm KE}|\ \boldsymbol{i};\Gamma,g_\Gamma\rangle\langle\boldsymbol{i};\Gamma,g_\Gamma|\hat{H}_{\rm KE}|n_2\rangle}{-E_\Gamma}|a_{1g}^{s_3},a_{1g}^{s_4}\rangle\langle n_2|, \tag{B1}$$

with $\sum_{n_2}=\sum_{s_1,s_2}\sum_{|n_2\rangle=|a_{1g}^{s_1},e_g^{g_e;s_2}\rangle,|e_g^{g_e;s_1},a_{1g}^{s_2}\rangle}$. Namely, we should calculate the contributions from every $|\boldsymbol{i};\Gamma,g_\Gamma\rangle$ to $(\hat{H}_{\rm exch}^{a_{1g}\text{-}e_g^{g_e}})_{\mathbf{12}}$ in the similar way for the second-order perturbation terms except taking care of the difference between $|a_{1g}^{s_1},a_{1g}^{s_2}\rangle$ and $|a_{1g}^{s_1},e_g^{g_e;s_2}\rangle$ or between $|a_{1g}^{s_1},a_{1g}^{s_2}\rangle$ and $|e_g^{g_e;s_1},a_{1g}^{s_2}\rangle$. The calculated result for $|\boldsymbol{i};\Gamma,g_\Gamma\rangle = |\boldsymbol{i};A_1\rangle$ becomes

$$-\frac{4}{27}\frac{(t_1+2t_2+2t_3)[\omega^{n(g_e)}(t_1-t_2-t_3)]}{U+2J'}[(\frac{1}{4}\hat{n}_{\mathbf{1}}\hat{o}_{\mathbf{2}}^{g_e}-\hat{\boldsymbol{s}}_{\mathbf{1}}\cdot\hat{\boldsymbol{so}}_{\mathbf{2}}^{g_e})+(\frac{1}{4}\hat{o}_{\mathbf{1}}^{g_e}\hat{n}_{\mathbf{2}}-\hat{\boldsymbol{so}}_{\mathbf{1}}^{g_e}\cdot\hat{\boldsymbol{s}}_{\mathbf{2}})]$$
$$+\frac{4}{9}\frac{t_{\rm odd}(t_1+2t_2+2t_3)\omega^{n(g_e)}}{U+2J'}[(\frac{1}{4}\hat{n}_{\mathbf{1}}\hat{o}_{\mathbf{2}}^{g_e}-\hat{\boldsymbol{s}}_{\mathbf{1}}\cdot\hat{\boldsymbol{so}}_{\mathbf{2}}^{g_e})-(\frac{1}{4}\hat{o}_{\mathbf{1}}^{g_e}\hat{n}_{\mathbf{2}}-\hat{\boldsymbol{so}}_{\mathbf{1}}^{g_e}\cdot\hat{\boldsymbol{s}}_{\mathbf{2}})]. \tag{B2}$$

As the case with the derivation of Eq. (85), we first calculated the finite terms of $\langle\boldsymbol{i};A_1|\hat{H}_{\rm KE}|a_{1g}^{s_1},e_g^{g_e;s_2}\rangle$ and $\langle\boldsymbol{i};A_1|\hat{H}_{\rm KE}|e_g^{g_e;s_1},a_{1g}^{s_2}\rangle$ for $\boldsymbol{i}=\mathbf{1},\mathbf{2}$ and $s_1,s_2=\uparrow,\downarrow$, and then expressed the contribution in terms of those matrix elements and the operators. Then, the calculated result for $\Gamma=E$ is

$$-[\frac{1}{27}\frac{(t_1-t_2-t_3)[\omega^{n(g_e)}(2t_1-2t_2+t_3)-6t_2]-9\omega^{m(g_e)}t_{\rm odd}^2}{U-J'}$$
$$+\frac{1}{9}\frac{(t_1-t_2-t_3)[\omega^{n(g_e)}(2t_1+2t_2+t_3)+2t_2]+3(\omega^{n(g_e)}-1)t_{\rm odd}^2}{U-J'}][(\frac{1}{4}\hat{n}_{\mathbf{1}}\hat{o}_{\mathbf{2}}^{g_e}-\hat{\boldsymbol{s}}_{\mathbf{1}}\cdot\hat{\boldsymbol{so}}_{\mathbf{2}}^{g_e})+(\frac{1}{4}\hat{o}_{\mathbf{1}}^{g_e}\hat{n}_{\mathbf{2}}-\hat{\boldsymbol{so}}_{\mathbf{1}}^{g_e}\cdot\hat{\boldsymbol{s}}_{\mathbf{2}})]$$
$$-[\frac{1}{9}\frac{t_{\rm odd}[\omega^{m(g_e)}(t_1-t_2)+(3-4\omega^{m(g_e)})t_3]}{U-J'}+\frac{1}{9}\frac{t_{\rm odd}[(1-\omega^{n(g_e)})(t_1-t_2)+(2\omega^{m(g_e)}-5)t_3]}{U-J'}]$$
$$\times[(\frac{1}{4}\hat{n}_{\mathbf{1}}\hat{o}_{\mathbf{2}}^{g_e}-\hat{\boldsymbol{s}}_{\mathbf{1}}\cdot\hat{\boldsymbol{so}}_{\mathbf{2}}^{g_e})-(\frac{1}{4}\hat{o}_{\mathbf{1}}^{g_e}\hat{n}_{\mathbf{2}}-\hat{\boldsymbol{so}}_{\mathbf{1}}^{g_e}\cdot\hat{\boldsymbol{s}}_{\mathbf{2}}), \tag{B3}$$

the calculated result for $\Gamma=T_1$ is

$$
\begin{aligned}
&-[\frac{1}{9}\frac{(t_1-t_2-t_3)[-\omega^{m(g_e)}(t_1-t_2)+t_3]+3(1-\omega^{m(g_e)})t_{\rm odd}^2}{U'-J_{\rm H}}+\frac{1}{9}\frac{(t_1-t_2-t_3)[-(t_1-t_2)+\omega^{m(g_e)}t_3]+3(\omega^{m(g_e)}-1)t_{\rm odd}^2}{U'-J_{\rm H}}]\\
&\times[(\frac{3}{4}\hat{n}_{\mathbf{1}}\hat{o}_{\mathbf{2}}^{g_e}+\hat{\boldsymbol{s}}_{\mathbf{1}}\cdot\hat{\boldsymbol{so}}_{\mathbf{2}}^{g_e})+(\frac{3}{4}\hat{o}_{\mathbf{1}}^{g_e}\hat{n}_{\mathbf{2}}+\hat{\boldsymbol{so}}_{\mathbf{1}}^{g_e}\cdot\hat{\boldsymbol{s}}_{\mathbf{2}})]\\
&-[\frac{1}{9}\frac{t_{\rm odd}[\omega^{n(g_e)}(2t_1+4t_2+7t_3)-(5t_1+t_2-5t_3)]}{U'-J_{\rm H}}+\frac{1}{9}\frac{t_{\rm odd}[\omega^{n(g_e)}(7t_1+5t_2+2t_3)+(5t_1+t_2-5t_3)]}{U'-J_{\rm H}}]\\
&\times[(\frac{3}{4}\hat{n}_{\mathbf{1}}\hat{o}_{\mathbf{2}}^{g_e}+\hat{\boldsymbol{s}}_{\mathbf{1}}\cdot\hat{\boldsymbol{so}}_{\mathbf{2}}^{g_e})-(\frac{3}{4}\hat{o}_{\mathbf{1}}^{g_e}\hat{n}_{\mathbf{2}}+\hat{\boldsymbol{so}}_{\mathbf{1}}^{g_e}\cdot\hat{\boldsymbol{s}}_{\mathbf{2}})],
\end{aligned}
\tag{B4}
$$

and the calculated result for $\Gamma = T_2$ is

$$
\begin{aligned}
&-\{\frac{2}{9}\frac{\omega^{n(g_e)}[-2(t_2+t_3)^2+t_{\rm odd}^2]}{U'+J_{\rm H}}+\frac{1}{9}\frac{(t_1+t_2+t_3)[-\omega^{m(g_e)}(t_1+t_2)-t_3]+(2-3\omega^{n(g_e)})t_{\rm odd}^2}{U'+J_{\rm H}}\\
&+\frac{1}{9}\frac{(t_1+t_2+t_3)[-(t_1+t_2)-\omega^{m(g_e)}t_3]-(2+5\omega^{n(g_e)})t_{\rm odd}^2}{U'+J_{\rm H}}\}[(\frac{1}{4}\hat{n}_{\mathbf{1}}\hat{o}_{\mathbf{2}}^{g_e}-\hat{\boldsymbol{s}}_{\mathbf{1}}\cdot\hat{\boldsymbol{so}}_{\mathbf{2}}^{g_e})+(\frac{1}{4}\hat{o}_{\mathbf{1}}^{g_e}\hat{n}_{\mathbf{2}}-\hat{\boldsymbol{so}}_{\mathbf{1}}^{g_e}\cdot\hat{\boldsymbol{s}}_{\mathbf{2}})]\\
&+\{\frac{2}{3}\frac{\omega^{n(g_e)}t_{\rm odd}(t_2+t_3)}{U'+J_{\rm H}}-\frac{1}{9}\frac{t_{\rm odd}[-\omega^{n(g_e)}(2t_2+3t_3)-(3t_1+t_2+3t_3)]}{U'+J_{\rm H}}-\frac{1}{9}\frac{t_{\rm odd}[\omega^{n(g_e)}(3t_1-t_2)+(3t_1+t_2+3t_3)]}{U'+J_{\rm H}}\}\\
&\times[(\frac{1}{4}\hat{n}_{\mathbf{1}}\hat{o}_{\mathbf{2}}^{g_e}-\hat{\boldsymbol{s}}_{\mathbf{1}}\cdot\hat{\boldsymbol{so}}_{\mathbf{2}}^{g_e})-(\frac{1}{4}\hat{o}_{\mathbf{1}}^{g_e}\hat{n}_{\mathbf{2}}-\hat{\boldsymbol{so}}_{\mathbf{1}}^{g_e}\cdot\hat{\boldsymbol{s}}_{\mathbf{2}}).
\end{aligned}
\tag{B5}
$$

Combining all the above contributions with Eq. (B1) and carrying out some algebra with the equality, such as $\omega^{m(g_e)}+\omega^{n(g_e)}=-1$, we finally obtain Eq. (97) with Eqs. (100)–(103).

Appendix C: Argument for the importance of the multiorbital properties and mirror-mixing effect

In this appendix, we argue the importance of the multiorbital properties and mirror-mixing effect in the DM interaction. For that argument, we focus on the first term of Eq. (114), i.e. $-D(\hat{S}_{\mathbf{1}}^y\hat{S}_{\mathbf{2}}^z-\hat{S}_{\mathbf{1}}^z\hat{S}_{\mathbf{2}}^y)$. This term shows two differences in comparison with the Heisenberg-type interaction: one is about whether the interaction is odd about some coordinates or even about all; the other is about whether the interaction is antisymmetric or symmetric. Those two properties distinguish the DM interaction from the Heisenberg-type interaction in general. To obtain the odd and antisymmetric superexchange interaction, the multiorbital properties become vital because only the interorbital hopping integral becomes odd about some coordinates (the intraorbital hopping integrals are even about all the coordinates). For the case of the first term of Eq. (114), we need the hopping integral behaving as an odd function about y and z and an even function about x. Such hopping integral is obtained by the hopping integral between the d_{xz} and d_{xy} orbitals because the d_{xz} and d_{xy} orbitals behave like xz and xy, respectively. Then, the odd dependence of this hopping integral can hold in the superexchange interactions if we use this odd number of times. Since we should use another hopping integral to put the electron moved by this back into the initial site, the combination of the odd-mirror hopping integral and even-mirror hopping integral is necessary. Furthermore, we need the SOC to put the electron back into the initial (ground-state) orbital (for the case considered in this paper, move from the $e_g^{\pm}$ orbital to the a_{1g} orbital). Thus, the multiorbital properties and mirror-mixing effect is important to obtain the DM interaction.

Appendix D: Details of the rough estimation of $\frac{D}{J^{\rm FM}-J^{\rm AF}}$

In this appendix, we see the details of how to obtain the results shown in Figs. 7(a)–(d). The results are obtained as follows. First, by setting $A=t_1+t_2+t_3$, $B=t_2+t_3$, $J'=J_{\rm H}$ and $U'=U-2J_{\rm H}$ in Eq. (115) and expanding D as the power series of $\frac{J_{\rm H}}{U}$ within the $O(\frac{J_{\rm H}}{U})$ terms, we express D as

$$
D=\frac{12\lambda_{LS}t_{\rm odd}}{9U\Delta_{\rm tri}}[(A-2B)+6A\frac{J_{\rm H}}{U}]. \tag{D1}
$$

Second, by combining this equation with Eq. (88), we obtain

$$\frac{D}{J^{\rm FM}-J^{\rm AF}}=\frac{3\lambda_{LS}t_{\rm odd}}{\Delta_{\rm tri}}\frac{(A-2B)+6\frac{J_{\rm H}}{U}}{(A+B)^2-2\frac{J_{\rm H}}{U}[(A-2B)^2+9t_{\rm odd}^2]}. \tag{D2}$$

Third, to understand the rough dependence of $\frac{D}{J^{\rm FM}-J^{\rm AF}}$ on $\frac{J_{\rm H}}{U}$ and $\frac{t_{\rm odd}}{A}$ or $\frac{t_{\rm odd}}{B}$, we consider four cases about A and B, i.e., $A\gg B$, $A\ll B$, $A\sim B$, and $A\sim -B$. Fourth, by calculating the leading terms of $\frac{D}{J^{\rm FM}-J^{\rm AF}}$ in each case, the leading terms in $A\gg B$, $A\ll B$, $A\sim B$, and $A\sim -B$ are given by

$$\frac{D}{J^{\rm FM}-J^{\rm AF}}=\frac{3\lambda_{LS}}{\Delta_{\rm tri}}\frac{t_{\rm odd}}{A}\frac{1+6\frac{J_{\rm H}}{U}}{1-2\frac{J_{\rm H}}{U}(1+9\frac{t_{\rm odd}^2}{A^2})}, \tag{D3}$$

$$\frac{D}{J^{\rm FM}-J^{\rm AF}}=-\frac{6\lambda_{LS}}{\Delta_{\rm tri}}\frac{t_{\rm odd}}{B}\frac{1}{1-2\frac{J_{\rm H}}{U}(4+9\frac{t_{\rm odd}^2}{A^2})}, \tag{D4}$$

$$\frac{D}{J^{\rm FM}-J^{\rm AF}}=-\frac{3\lambda_{LS}}{2\Delta_{\rm tri}}\frac{t_{\rm odd}}{B}\frac{1-6\frac{J_{\rm H}}{U}}{2-\frac{J_{\rm H}}{U}(1+9\frac{t_{\rm odd}^2}{A^2})}, \tag{D5}$$

and

$$\frac{D}{J^{\rm FM}-J^{\rm AF}}=\frac{\lambda_{LS}}{6\Delta_{\rm tri}}\frac{t_{\rm odd}}{B}\frac{1+2\frac{J_{\rm H}}{U}}{\frac{J_{\rm H}}{U}(1+\frac{t_{\rm odd}^2}{A^2})}, \tag{D6}$$

respectively. By using those equations and setting $\lambda_{LS}=0.03$ eV and $\Delta_{\rm tri}=1$ eV, we obtain the results shown in Figs. 7(a)–(d).

Appendix E: Derivation of Eq. (116)

In this appendix, we derive Eq. (116). For this derivation, we first rewrite the third term of Eq. (93) for sublattices 1 and 2 as

$$(\hat{H}^{\rm KE-}_{\rm 3rd}{}^{LS-{\rm KE}})_{\mathbf{12}}\approx\sum_{\boldsymbol{i}=\mathbf{1},\mathbf{2}}\sum_{\Gamma,\Gamma'(\neq\Gamma)}\sum_{g_\Gamma,g_{\Gamma'}}\sum_{s_1,s_2,s_3,s_4}\times\frac{\langle a_{1g}^{s_3},a_{1g}^{s_4}|\hat{H}_{\rm KE}|\boldsymbol{i};\Gamma,g_\Gamma\rangle}{-E_\Gamma}\langle\boldsymbol{i};\Gamma,g_\Gamma|\hat{H}_{LS}|\boldsymbol{i};\Gamma',g_{\Gamma'}\rangle\times\frac{\langle\boldsymbol{i};\Gamma',g_{\Gamma'}|\hat{H}_{\rm KE}|a_{1g}^{s_1},a_{1g}^{s_2}\rangle}{-E_{\Gamma'}}|a_{1g}^{s_3},a_{1g}^{s_4}\rangle\langle a_{1g}^{s_1},a_{1g}^{s_2}|. \tag{E1}$$

This shows that $(\hat{H}^{\rm KE-}_{\rm 3rd}{}^{LS-{\rm KE}})_{\mathbf{12}}$ for our model can be derived by combining the contributions from every term of $|\boldsymbol{i};\Gamma',g_{\Gamma'}\rangle$. Those contributions can be calculated by using the matrix elements, $\langle a_{1g}^{s_3},a_{1g}^{s_4}|\hat{H}_{\rm KE}|\boldsymbol{i};\Gamma,g_\Gamma\rangle$ and $\langle\boldsymbol{i};\Gamma',g_{\Gamma'}|\hat{H}_{\rm KE}|a_{1g}^{s_1},a_{1g}^{s_2}\rangle$, which have been calculated in the second-order perturbation terms, and the matrix element, $\langle\boldsymbol{i};\Gamma,g_\Gamma|\hat{H}_{LS}|\boldsymbol{i};\Gamma',g_{\Gamma'}\rangle$, which is obtained by using the relation, such as Eqs. (78)–(81). Namely, the contribution from $|\boldsymbol{i};\Gamma',g_{\Gamma'}\rangle=|\boldsymbol{i};A_1\rangle$ is

$$\frac{2}{9}\frac{\lambda_{LS}t_{\rm odd}(t_1+2t_2+2t_3)}{(U'-J_{\rm H})(U+2J')}\{(1-i)[(\frac{1}{2}\hat{n}_{\mathbf{1}}+\hat{s}_{\mathbf{1}}^z)\hat{s}_{\mathbf{2}}^+-s_{\mathbf{1}}^+(\frac{1}{2}\hat{n}_{\mathbf{2}}+\hat{s}_{\mathbf{2}}^z)]+(1+i)[\hat{s}_{\mathbf{1}}^-(\frac{1}{2}\hat{n}_{\mathbf{2}}-\hat{s}_{\mathbf{2}}^z)-(\frac{1}{2}\hat{n}_{\mathbf{1}}-\hat{s}_{\mathbf{1}}^z)\hat{s}_{\mathbf{2}}^-]\}, \tag{E2}$$

the contribution from $|\boldsymbol{i};\Gamma',g_{\Gamma'}\rangle=|\boldsymbol{i};E,u\rangle$ is

$$\frac{1}{9}\frac{i\lambda_{LS}t_{\rm odd}(t_1-t_2-t_3)}{(U'-J_{\rm H})(U-J')}[(\frac{1}{2}\hat{n}_{\mathbf{1}}+\hat{s}_{\mathbf{1}}^z)\hat{s}_{\mathbf{2}}^+-\hat{s}_{\mathbf{1}}^+(\frac{1}{2}\hat{n}_{\mathbf{2}}+\hat{s}_{\mathbf{2}}^z)+(\frac{1}{2}\hat{n}_{\mathbf{1}}-\hat{s}_{\mathbf{1}}^z)\hat{s}_{\mathbf{2}}^--\hat{s}_{\mathbf{1}}^-(\frac{1}{2}\hat{n}_{\mathbf{2}}-\hat{s}_{\mathbf{2}}^z)]$$
$$+\frac{2}{9}\frac{\lambda_{LS}t_{\rm odd}(t_1-t_2-t_3)}{(U'-J_{\rm H})(U-J')}[(\frac{1}{2}\hat{n}_{\mathbf{1}}+\hat{s}_{\mathbf{1}}^z)\hat{s}_{\mathbf{2}}^+-\hat{s}_{\mathbf{1}}^+(\frac{1}{2}\hat{n}_{\mathbf{2}}+\hat{s}_{\mathbf{2}}^z)-(\frac{1}{2}\hat{n}_{\mathbf{1}}-\hat{s}_{\mathbf{1}}^z)\hat{s}_{\mathbf{2}}^-+\hat{s}_{\mathbf{1}}^-(\frac{1}{2}\hat{n}_{\mathbf{2}}-\hat{s}_{\mathbf{2}}^z)], \tag{E3}$$

the contribution from $|\boldsymbol{i};\Gamma',g_{\Gamma'}\rangle=|\boldsymbol{i};E,v\rangle$ is

$$-\frac{1}{3}\frac{i\lambda_{LS}t_{\rm odd}(t_1-t_2-t_3)}{(U'-J_{\rm H})(U-J')}[(\frac{1}{2}\hat{n}_{\mathbf{1}}+\hat{s}_{\mathbf{1}}^z)\hat{s}_{\mathbf{2}}^+-\hat{s}_{\mathbf{1}}^+(\frac{1}{2}\hat{n}_{\mathbf{2}}+\hat{s}_{\mathbf{2}}^z)+(\frac{1}{2}\hat{n}_{\mathbf{1}}-\hat{s}_{\mathbf{1}}^z)\hat{s}_{\mathbf{2}}^--\hat{s}_{\mathbf{1}}^-(\frac{1}{2}\hat{n}_{\mathbf{2}}-\hat{s}_{\mathbf{2}}^z)], \tag{E4}$$

the contribution from $|\boldsymbol{i};\Gamma',g_{\Gamma'}\rangle=|\boldsymbol{i};T_1,\xi_\pm\rangle$ is

$$[\frac{2}{9}\frac{i\lambda_{LS}t_{\rm odd}(t_1+2t_2+2t_3)}{(U+2J')(U'-J_{\rm H})}-\frac{1}{9}\frac{i\lambda_{LS}t_{\rm odd}(t_1-t_2-t_3)}{(U-J')(U'-J_{\rm H})}+\frac{1}{3}\frac{i\lambda_{LS}t_{\rm odd}(t_1-t_2-t_3)}{(U-J')(U'-J_{\rm H})}\pm\frac{1}{9}\frac{\lambda_{LS}t_{\rm odd}(-t_1+4t_2+4t_3)}{(U'+J_{\rm H})(U'-J_{\rm H})}]$$
$$\times[(\frac{1}{2}\hat{n}_{\mathbf{1}}\pm\hat{s}_{\mathbf{1}}^z)\hat{s}_{\mathbf{2}}^\mp-\hat{s}_{\mathbf{1}}^\mp(\frac{1}{2}\hat{n}_{\mathbf{2}}\pm\hat{s}_{\mathbf{2}}^z)], \tag{E5}$$

the contribution from $|\boldsymbol{i};\Gamma',g_{\Gamma'}\rangle=|\boldsymbol{i};T_1,\eta_\pm\rangle$ is

$$[\frac{2}{9}\frac{\lambda_{LS}t_{\rm odd}(t_1+2t_2+2t_3)}{(U+2J')(U'-J_{\rm H})}+\frac{2}{9}\frac{\lambda_{LS}t_{\rm odd}(t_1-t_2-t_3)}{(U-J')(U'-J_{\rm H})}\pm\frac{1}{9}\frac{i\lambda_{LS}t_{\rm odd}(-t_1+4t_2+4t_3)}{(U'+J_{\rm H})(U'-J_{\rm H})}][\pm(\frac{1}{2}\hat{n}_{\mathbf{1}}\pm\hat{s}_{\mathbf{1}}^z)\hat{s}_{\mathbf{2}}^\mp\mp\hat{s}_{\mathbf{1}}^\mp(\frac{1}{2}\hat{n}_{\mathbf{2}}\pm\hat{s}_{\mathbf{2}}^z)], \tag{E6}$$

the contribution from $|\boldsymbol{i};\Gamma',g_{\Gamma'}\rangle=|\boldsymbol{i};T_2,\zeta_0\rangle$ is

$$\frac{1}{9}\frac{\lambda_{LS}t_{\rm odd}(-t_1+4t_2+4t_3)}{(U'-J_{\rm H})(U'+J_{\rm H})}\{(1-i)[(\frac{1}{2}\hat{n}_{\boldsymbol{1}}+\hat{s}^z_{\boldsymbol{1}})\hat{s}^+_{\boldsymbol{2}}-\hat{s}^+_{\boldsymbol{1}}(\frac{1}{2}\hat{n}_{\boldsymbol{2}}+\hat{s}^z_{\boldsymbol{2}})]+(1+i)[\hat{s}^-_{\boldsymbol{1}}(\frac{1}{2}\hat{n}_{\boldsymbol{2}}-\hat{s}^z_{\boldsymbol{2}})-(\frac{1}{2}\hat{n}_{\boldsymbol{1}}-\hat{s}^z_{\boldsymbol{1}})\hat{s}^-_{\boldsymbol{2}}]\}, \quad \text{(E7)}$$

the contribution from $|\boldsymbol{i};\Gamma',g_{\Gamma'}\rangle=|\boldsymbol{i};T_1,\xi_0\rangle$ is

$$\frac{1}{9}\frac{i\lambda_{LS}t_{\rm odd}(2t_1+t_2+t_3)}{(U'+J_{\rm H})(U'-J_{\rm H})}[(\frac{1}{2}\hat{n}_{\boldsymbol{1}}+\hat{s}^z_{\boldsymbol{1}})(\frac{1}{2}\hat{n}_{\boldsymbol{2}}-\hat{s}^z_{\boldsymbol{1}})+\hat{s}^+_{\boldsymbol{1}}\hat{s}^-_{\boldsymbol{2}}-\hat{s}^-_{\boldsymbol{1}}\hat{s}^+_{\boldsymbol{2}}-(\frac{1}{2}\hat{n}_{\boldsymbol{1}}-\hat{s}^z_{\boldsymbol{1}})(\frac{1}{2}\hat{n}_{\boldsymbol{2}}+\hat{s}^z_{\boldsymbol{2}})], \quad \text{(E8)}$$

the contribution from $|\boldsymbol{i};\Gamma',g_{\Gamma'}\rangle=|\boldsymbol{i};T_2,\xi_0\rangle$ is

$$\frac{1}{9}\frac{i\lambda_{LS}t_{\rm odd}(2t_1+t_2+t_3)}{(U'+J_{\rm H})(U'-J_{\rm H})}[(\frac{1}{2}\hat{n}_{\boldsymbol{1}}+\hat{s}^z_{\boldsymbol{1}})(\frac{1}{2}\hat{n}_{\boldsymbol{2}}-\hat{s}^z_{\boldsymbol{1}})-\hat{s}^+_{\boldsymbol{1}}\hat{s}^-_{\boldsymbol{2}}+\hat{s}^-_{\boldsymbol{1}}\hat{s}^+_{\boldsymbol{2}}-(\frac{1}{2}\hat{n}_{\boldsymbol{1}}-\hat{s}^z_{\boldsymbol{1}})(\frac{1}{2}\hat{n}_{\boldsymbol{2}}+\hat{s}^z_{\boldsymbol{2}})], \quad \text{(E9)}$$

the contribution from $|\boldsymbol{i};\Gamma',g_{\Gamma'}\rangle=|\boldsymbol{i};T_1,\eta_0\rangle$ is

$$-\frac{1}{9}\frac{i\lambda_{LS}t_{\rm odd}(2t_1+t_2+t_3)}{(U'+J_{\rm H})(U'-J_{\rm H})}[(\frac{1}{2}\hat{n}_{\boldsymbol{1}}+\hat{s}^z_{\boldsymbol{1}})(\frac{1}{2}\hat{n}_{\boldsymbol{2}}-\hat{s}^z_{\boldsymbol{1}})+\hat{s}^+_{\boldsymbol{1}}\hat{s}^-_{\boldsymbol{2}}-\hat{s}^-_{\boldsymbol{1}}\hat{s}^+_{\boldsymbol{2}}-(\frac{1}{2}\hat{n}_{\boldsymbol{1}}-\hat{s}^z_{\boldsymbol{1}})(\frac{1}{2}\hat{n}_{\boldsymbol{2}}+\hat{s}^z_{\boldsymbol{2}})], \quad \text{(E10)}$$

the contribution from $|\boldsymbol{i};\Gamma',g_{\Gamma'}\rangle=|\boldsymbol{i};T_2,\eta_0\rangle$ is

$$-\frac{1}{9}\frac{i\lambda_{LS}t_{\rm odd}(2t_1+t_2+t_3)}{(U'+J_{\rm H})(U'-J_{\rm H})}[(\frac{1}{2}\hat{n}_{\boldsymbol{1}}+\hat{s}^z_{\boldsymbol{1}})(\frac{1}{2}\hat{n}_{\boldsymbol{2}}-\hat{s}^z_{\boldsymbol{1}})-\hat{s}^+_{\boldsymbol{1}}\hat{s}^-_{\boldsymbol{2}}+\hat{s}^-_{\boldsymbol{1}}\hat{s}^+_{\boldsymbol{2}}-(\frac{1}{2}\hat{n}_{\boldsymbol{1}}-\hat{s}^z_{\boldsymbol{1}})(\frac{1}{2}\hat{n}_{\boldsymbol{2}}+\hat{s}^z_{\boldsymbol{2}})], \quad \text{(E11)}$$

and the contributions from $|\boldsymbol{i};\Gamma',g_{\Gamma'}\rangle=|\boldsymbol{i};T_1,\zeta_\pm\rangle,|\boldsymbol{i};T_1,\zeta_0\rangle$ are zero for $(\hat{H}^{\rm KE-}_{\rm 3rd}{}^{LS-{\rm KE}})_{\boldsymbol{12}}$. Combining those results with Eq. (E1), we obtain Eq. (116) with Eq. (117).

* Electronic address: arakawa@hosi.phys.s.u-tokyo.ac.jp

1 J. S. Gardner, M. J. P. Gingras, and J. E. Greedan, Rev. Mod. Phys. **82**, 53 (2010).
2 S. Kondo, D. C. Johnston, C. A. Swenson, F. Borsa, A. V. Mahajan, L. L. Miller, T. Gu, A. I. Goldman, M. B. Maple, D. A. Gajewski, E. J. Freeman, N. R. Dilley, R. P. Dickey, J. Merrin, K. Kojima, G. M. Luke, Y. J. Uemura, O. Chmaissem and J. D. Jorgensen, Phys. Rev. Lett. **78**, 3729 (1997).
3 Y. Onose, T. Ideue, H. Katsura, Y. Shiomi, N. Nagaosa and Y. Tokura, Science **329**, 297 (2010).
4 J. Matsuno, A. Fujimori and L. F. Mattheiss, Phys. Rev. B **60**, 1607 (1999).
5 V. I. Anisimov, M. A. Korotin, M. Zölfl, T. Pruschke, K. Le Hur and T. M. Rice, Phys. Rev. Lett. **83**, 364 (1999).
6 H. J. Xiang, E. J. Kan, M.-H. Whangbo, C. Lee, Su-Huai Wei and X. G. Gong, Phys. Rev. B **83**, 174402 (2011).
7 I. Dzyaloshinsky, J. Phys. Chem. Solids **4**, 241 (1958).
8 T. Moriya, Phys. Rev. Lett. **4**, 228 (1960); T. Moriya, Phys. Rev. **120**, 91 (1960).
9 M. Elhajal, B. Canals, R. Sunyer and C. Lacroix, Phys. Rev. B **71**, 094420 (2005).
10 M. Mena, R. S. Perry, T. G. Perring, M. D. Le, S. Guerrero, M. Storni, D. T. Adroja, Ch. Rüegg and D. F. McMorrow, Phys. Rev. Lett. **113**, 047202 (2014).
11 K. Riedl, D. Guterding, H. O. Jeschke, M. J. P. Gingras and R. Valentí, Phys. Rev. B **94**, 014410 (2016).
12 J.-H. Chung, M. Matsuda, S.-H. Lee, K. Kakurai, H. Ueda, T. J. Sato, H. Takagi, K.-P. Hong, and S. Park, Phys. Rev. Lett. **95**, 247204 (2005).
13 Gia-Wei Chern, C. J. Fennie, and O. Tchernyshyov, Phys. Rev. B **74**, 060405(R) (2006).
14 C. Donnerer, M.C. Rahn, M. Moretti Sala, J.G. Vale, D. Pincini, J. Strempfer, M. Krisch, D. Prabhakaran, A.T. Boothroyd, and D.F. McMorrow, Phys. Rev. Lett. **117**, 037201 (2016).
15 R. Matsumoto, and S. Murakami, Phys. Rev. B **84**, 184406 (2011).
16 T. Ideue, Y. Onose, H. Katsura, Y. Shiomi, S. Ishiwata, N. Nagaosa and Y. Tokura, Phys. Rev. B **85** (2012) 134411.
17 N. Arakawa, arXiv:1604.05867.
18 H. Tsunetsugu, J. Phys. Soc. Jpn. **71** (2002) 1844.
19 Y. Yamashita and K. Ueda, Phys. Rev. B **67**, 195107 (2003).
20 K. Hattori and H. Tsunetsugu, Phys. Rev. B **79**, 035115 (2009).
21 B.-J. Yang and Y. B. Kim, Phys. Rev. B **82**, 085111 (2010).
22 H. Ichikawa, L. Kano, M. Saitoh, S. Miyahara, N. Furukawa, J. Akimitsu, T. Yokoo, T. Matsumura, M. Takeda and K. Hirota, J. Phys. Soc. Jpn. **74**, 1020 (2005).
23 J. C. Slater and G. F. Koster, Phys. Rev. **94**, 1498 (1954).
24 Y. Yanase, J. Phys. Soc. Jpn. **82**, 044711 (2013).
25 T. Mizoguchi and N. Arakawa, Phys. Rev. B **93**, 041304(R) (2016).
26 E. I. Rashba, Fizika Tverd. Tela, **2**, 1224 (1960) [Sov. Phys. Solid State **2**, 1109 (1960)].
27 For the spin-gauge potential, e.g., see Y. Tokura, S. Seki, and N. Nagaosa, Rep. Prog. Phys. **77**, 076501 (2014).

[28] P. W. Anderson, Phys. Rev. **115**, 2 (1959).
[29] J. J. Sakurai, *Modern Quantum Mechanics* (Benjamin/Cummings, Menlo park, 1985).
[30] W. A. Harrison, *Electronic Structure and the Properties of Solids* (Dover Publication, INC., New York, 1989).
[31] S.-H. Lee, C. Broholm, T. H. Kim, W. Ratcliff II, and S-W. Cheong, Phys. Rev. Lett. **84**, 3718 (2000).